Journal of Engineering, Science and Technological Trends (JESTT)

Vol. 3, Issue 1, March 2026
DOI: https://doi.org/10.64060/jestt.v3i1.6

Review

# Green-Synthesized Carbon Quantum Dots for Environmental Monitoring of Heavy Metals: A Critical Review of Mechanisms and Performance

Muhammad Arslan Akhtar [1]†, Jalwa Anum [1]†, Abdul Rehman [2] and Rabia [3]

[1]Department of Chemistry, COMSATS University Islamabad, Pakistan
[2]School of Chemical Engineering and Technology, Institute of Molecular Plus, Tianjin University, Tianjin 300072, China
[3]Institute of Molecular Aggregation Science, Tianjin University, Tianjin 300072 China
* Corresponding Email: arslanimran042@gmail.com (M. A. Akhtar), † Equally contributed and share first authorship.

Received: 05 January 2026 / Revised: 13 February 2026 / Accepted: 22 February 2026 / Published online: 01 March 2026



## ABSTRACT

The heavy-metal contamination of water bodies is still a crucial environmental issue and a hazard to the ecosystem as well as human health, and incomplete knowledge of how the synthesis of carbon quantum dots (CQD) can regulate the analytical performance of sensing technologies. Despite the benefits of CQDs reported in many studies, systemic linkages between preparation strategy, surface chemistry, photophysical behaviour, and sensing efficiency are yet to be explained well. This review presents a critical argument of the green bottom-up strategies to fabricate CQDs and compares them to the top-down methods in order to understand the way precursor selection, the introduction of heteroatoms, and the control of defects affect quantum yield, emission mechanisms, and environmental friendliness. The special focus is put on the fluorescence modulation mechanisms such as photoinduced electron transfer, Förster/energy transfer, inner filter effects and static versus dynamic quenching and their application in the detection of priority pollutants, including Pb(II), Hg(II), Cu(II), Cr(V) and Fe(III). In addition to publishing literature research, we compare reported detection limits, linear working ranges and selectivity factors to derive general performance patterns. The analysis has shown that controlled surface passivation and functional groups are the final determinants towards sub-micromolar sensitivity and better anti-interference properties. Other issues raised regarding reproducibility, complexity of real-world samples, long-term stability and scalable green production are also addressed. Combining synthesis-structure-property-performance correlations, this review develops empirical design guidelines of the next-generation CQD sensors and explains feasible ways of developing sustainable monitoring and mitigation of heavy-metal pollution in the environment.

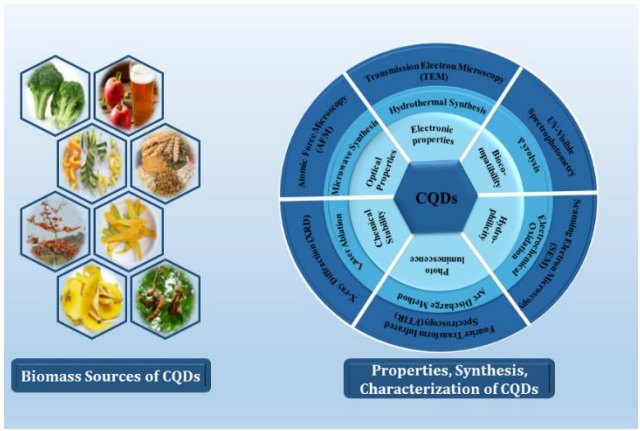


**Keywords**: CQD: Carbon Quantum Dots; Environmental Monitoring; Fluorescence Quenching; Green Synthesis; Heavy Metal Detection

## 1. Introduction

Carbon-based nanostructures have emerged as an important class of materials due to their diverse physicochemical properties and broad technological relevance. Materials such as graphene, carbon nanotubes, fullerenes, and nanodiamonds have been extensively investigated [1]; however, their practical implementation is often restricted by intrinsic limitations. In particular, poor aqueous dispersibility and weak visible-region emission hinder the use of graphene and fullerenes, while nanodiamonds suffer from complex synthesis, purification, and size-control challenges [2],[3]. These limitations have driven the search for alternative carbon nanomaterials (NMs) that combine strong fluorescence, water compatibility, and sustainable

production. In this context, fluorescent carbon dots have gained prominence as a new generation of carbon-based NMs capable of overcoming the drawbacks associated with conventional carbon nanostructures [4].

Carbon quantum dots CQDs were first discovered by Xu et al. during the purification of single-walled carbon nanotubes (CNTs) [5]. Since then, CQDs have gained significant interest due to their nanoscale size (<10 nm), quasi-spherical morphology, excellent water solubility, and highly tunable photoluminescence [6]. Structurally, CQDs consist of an amorphous or partially crystalline $sp^2/sp^3$ hybridized carbon core decorated with abundant oxygen- and nitrogen-containing surface functional groups such as hydroxyl, carboxyl, and amine moieties. These surface groups, which vary depending on the precursor and synthesis route, play a crucial role in governing their optical behaviour, solubility, and sensing performance [7].

Compared with traditional semiconductor quantum dots such as CdTe, CdS, and CdSe, which exhibit superior optical properties but suffer from toxicity, high cost, and limited biocompatibility, CQDs offer distinct advantages, including low toxicity, chemical stability, excellent aqueous dispersibility, and compatibility with biological systems [8],[9]. These features make CQDs particularly attractive for environmental and biomedical applications. Furthermore, heteroatom doping (e.g., N, S, P) has been shown to significantly enhance their fluorescence efficiency, charge transfer behaviour, and metal ion affinity [10].

In recent years, increasing emphasis has been placed on the sustainable and green synthesis of CQDs, particularly via bottom-up approaches using renewable biomass precursors. Biomass sources such as plant waste, agricultural residues, algae, animal waste, and industrial by-products provide an abundant, low-cost, and environmentally benign carbon source for CQD production [11],[12]. The inherent presence of heteroatoms and functional groups in biomass facilitates carbonisation and surface passivation without the need for harsh chemicals. CQDs derived from biomass exhibit excellent biocompatibility, non-toxicity, and photostability, making them superior alternatives to chemically synthesised counterparts [13],[14].

Among the various applications of CQDs, heavy metal ion sensing has emerged as one of the most extensively explored areas. Owing to their strong fluorescence, high quantum yield, and surface-rich functional chemistry, CQDs enable sensitive and selective detection of toxic metal ions even at trace levels [15],[16]. Their excellent photostability ensures reliable signal output, which is essential for accurate monitoring of water quality. However, challenges such as post-synthetic functionalization, purification complexity, and detailed structural characterisation remain and must be addressed for large-scale deployment [17].

Photoinduced electron transfer, energy transfer routes and inner filter effects are often the most popular ways of mechanistically interpreting fluorescence modulation, and are often described independently of structural evidence. This means that practical design guidelines towards creating a dependable and repeatable CQD sensor are yet to be developed.

This review highlights recent advancements toward the sustainable production of fluorescent CQDs, with a primary focus on eco-friendly bottom-up synthesis routes, including hydrothermal, microwave-assisted, and carbonisation methods using biomass precursors. In addition, the review critically discusses the application of CQDs as fluorescent probes for selective heavy metal detection in aqueous medium, emphasising sensing mechanisms, material performance, and prospects in environmental remediation.

## 2. Synthesis of CQDs

After Xu and his colleagues' accidental discovery of CQDs in 2004 during the purification of single-walled carbon nanotubes, different methods have been introduced to synthesise CQDs, as shown in Figure 1 [18] (Table 1). These approaches can be categorised as Top-down and Bottom-up. The top-down approach involves the production of Nano-sized particles through the breakdown of larger carbon precursors like graphene, ash, or soot via arc discharge [19], chemical oxidation, laser ablation [20], electrochemical oxidation, etc. Unfortunately, this method has some disadvantages, such as the need for pricey components, difficult reaction conditions, and a lengthy reaction time. Likewise, the ‘‘bottom-up’’ methodology generates CQDs from less expensive precursors utilising straightforward experimental setups, negating the need for complex methods and expensive precursors [21]. The bottom-up refers to the process of creating

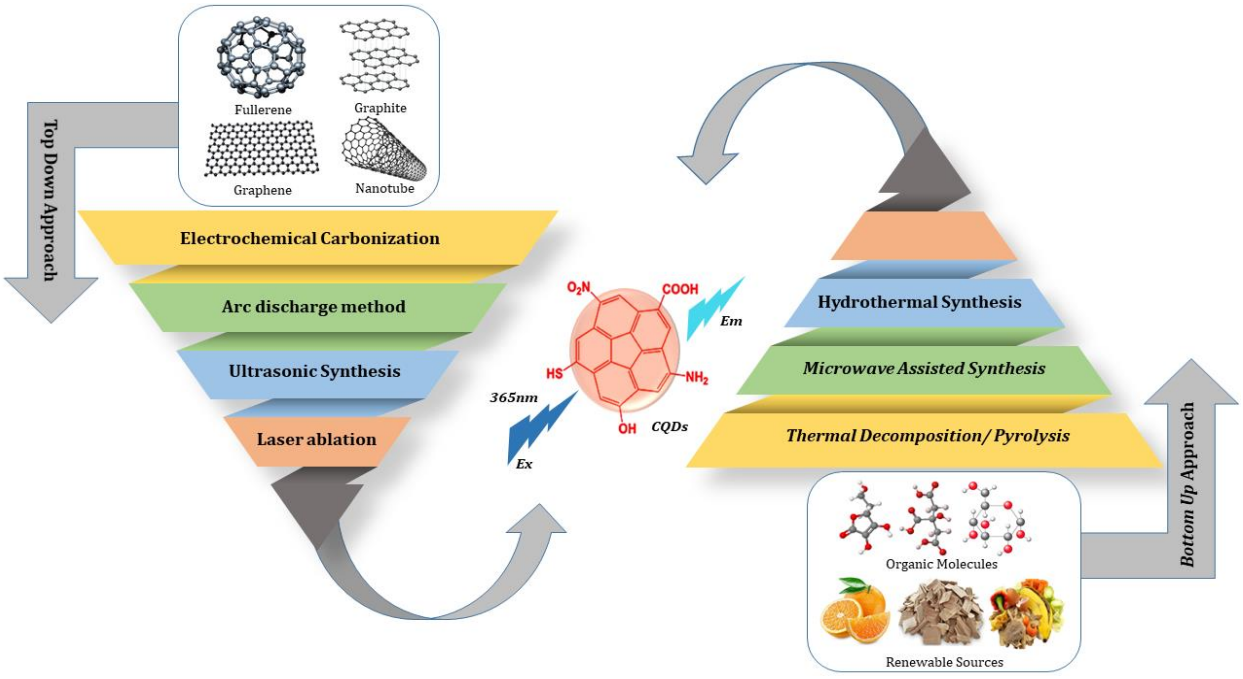


**Figure 1:** *Carbon Quantum Dot Fabrication via Top-Down and Bottom-Up Strategies*

huge nanostructures using energy from smaller carbon components such as amino acids, polymers, carbohydrates, and waste materials combined to form CQDs via chemical reactions, such as hydrothermal reaction, chemical solution synthesis, pyrolysis, microwave assistance, ultrasonic methods, and template-based routes or plasma treatment [22].

Choosing appropriate carbon precursors is the initial stage in the bottom-up process, and it directly impacts the properties of the final CQDs. In the second stage, the chosen carbon precursor is carbonised, and any impurities that may have formed during the carbonisation process are then purified. Precursors with carboxyl and hydroxyl functional groups on their surface are appropriate for the production of CQDs. schematic representation of various routes The scientific community has taken notice of the green approach to the CQDs synthesis because of its non-hazardous character. Utilising green resources as a carbon source is necessary. The raw materials and synthesis techniques significantly influence the features of colloidal quantum dots, such as size, colloidal stability, compatibility, functional groups, fluorescence properties, quantum yield (QY), and crystallinity. The green methods for creating CQDs are covered in the following section. The carbonisation, hydrothermal, and microwave-aided processes are mostly explored to synthesise CQDs from green precursors, primarily biomass as the raw material [23].

## 3. Transition to Green Synthesis Methods

This section focuses on the eco-friendly approach towards the fabrication of CQDs. These environmentally friendly methods not only solve environmental issues but also reduce the presence of toxic components, improve environmental and public health safety, employ a low-cost synthesis procedure, and promote sustainability.

### 3.1. Hydrothermal Method

Hydrothermal synthesis is one of the most frequent, non-toxic, and affordable ways to prepare CQDs. It is primarily a solution-reaction-based method that utilises precursors such as biomass saccharides, organic acids, juices, and waste peels. The primary benefit of this method is that it is a reasonably easy and 'green' process, making it environmentally benign and less harmful, with an evenly sized distribution of synthesised CQDs that are extremely efficient [24]. In a simple one-step hydrothermal process, the target precursor solution is heated in an autoclave reactor with Teflon lining to conduct the hydrothermal reaction at high pressure and high temperature, as shown in Figure 2 [25]. HTC has been reported for the synthesis of self-passivated fluorescent CQDs in one step using reagents such as glucose, citric acid, ascorbic acid [26], biomass waste (mango peels, soy milk, broccoli [27], lemon juice, banana peel [28], honey-comb, cambuci juice [29], starch [30], cellulose [31] and paper as carbon source [32]. The reaction can be carried out in an aqueous or organic solvent. Solvothermal carbonisation with subsequent organic solvent extraction is a prevalent method for synthesising CQDs. Carbon precursors are thermally treated in high-boiling-point solvents, then extracted and concentrated. Bhunia et al produced hydrophobic and hydrophilic CQDs under 10 nm from carbohydrates. Hydrophobic CQDs were synthesised by heating a carbohydrate, octadecylamine, and octadecene mixture at 70-300c for 10-30 minutes. Hydrophilic CQDs were generated by heating an aqueous carbohydrate solution across various pH levels or with phosphoric acid at 80-90c for 60 minutes [33]. Lu, Zifan, et al. prepared n-CQD with yellow-green fluorescence by surface functionalization of CQDs via solvothermal method. The prepared N-CQDs showed a considerable QY (5.11%) and high chemical and optical stability. More importantly, N-CQDs showed good selectivity and sensitivity to $Ag^{+}$ at the concentrations of 0–10 μM and 10–30 μM, respectively. N-CQDs were used to detect the content of $Ag^{+}$ in food packaging material [34]. Singh, Harpreet, et al. proposed fluorescent CQDs from cabbage (2-4 nm), whose fluorescence was suppressed upon reaction with $Fe^{3+}$, $Pb^{2+}$, and $Hg^{2+}$ ions [35]. These CQDs work well for heavy metal detection, although more research work is required to improve selectivity and quantitative analysis. Functionalizing CQDs with specific ligands

**Table 1**
Advantages and disadvantages of Top-Down and Bottom-Up approaches [21]

| Methods | Advantages | Disadvantages |
|---|---|---|
| **Top-down** | • Raw materials are used efficiently by breaking down carbon sources into smaller fragments<br>• Utilizes readily available and inexpensive carbon sources like carbon nanotubes, graphite, and carbon soot.<br>• Controls size, shape, and surface functionalities of CQDs by selecting precursors and reaction conditions.<br>• One-step manufacturing can control over size of the nanostructure with excellent product quality. | • Thus, severe conditions of the reaction, for example, using large concentrations of acids or oxidants, high temperature, and long-time of reaction<br>• Newly produced CQDs have poor control over their size distribution and surface functionalities.<br>• Such a pattern may produce structural defects and impurities, while the synthesis procedure's batch nature may hinder scalability.<br>• One disadvantage is that there may be some oxidation or by-product formations and hence the final product may be contaminated. |
| **Bottom-up** | • Reaction conditions are milder than top-down methods, which typically involve microwave or hydrothermal processes.<br>• Nanostructures with fewer defects and a more uniform chemical composition. Heteroatoms can be introduced during synthesis.<br>Potential for large-scale production, high reproducibility, simple processes, improved performance, and environmentally friendly characteristics | • The task here is to attain homogeneity in size and at the same time manage surface activity.<br>• The top-down methods are elaborate and provide a restricted number of carbon sources to work on. |

may enhance their specificity [35]. Nan, Zhezhu, et al. effectively created a detection method for Ferric iron (Fe (III)) using CQDs modified ZnO/CdS nanoparticles. The interaction between Fe(III) and CQDs/ZnO/CdS NPs led to efficient fluorescence quenching. Moreover, the Fe(III) detection limit was determined to be approximately 1:72 $\times 10^{-7}$ M. [36] Khan, Zubair MSH, et al. successfully synthesized blue fluorescent NCQDs with a quantum yield of 13.2%. this N-CQDs works as a nanoprobe sensor for selective and sensitive detection of $Fe^{3+}$ with as low as 0.10 µM concentration of $Fe^{3+}$ can be detected in the linear range of 2–20 µM. [37] Similarly, Aygun, Aysenur, et al. synthesize CQDs doped with heteroatoms such as sulfur, nitrogen, and boron (N-CQD, B-CQD, and S-CQD) with average sizes in the range of 5–7 nm as colorimetric sensors for heavy metals successfully. It was observed that CQDs detected $Fe^{3+}$ metal ions, B-CQD and S-CQD detected $Fe^{3+}$ and $Ag^{+}$ metal ions, and N-CQDs detected $Ca^{2+}$ metal ions with different LOD values for different metals [38]. Kolaprath, Mrinalini Kalyani Ayilliath, Libina Benny, and Anitha Varghese. Synthesized CQDs from the leaves of Polyalthia longifolia (a natural source) through a one-step hydrothermal method with a QY of 22% and an average size of 3.33 nm. The p-CQDs showed high sensitivity, selectivity, and a low detection limit of 2.4 nM for the determination of $Cd^{2+}$ ions [39].

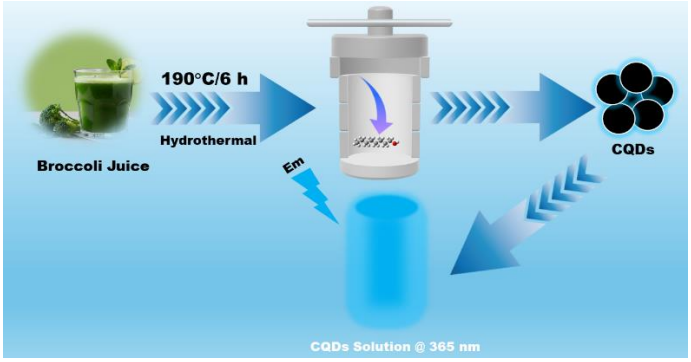


**Figure 2:** *Biomass-Derived CQDs: Hydrothermal Transformation of Broccoli Juice [27]*

### 3.2. Microwave Assisted Synthesis

Microwave pyrolysis, which is one of the satisfactory and efficient bottom-up methods, has been used for synthesising CQDs. This technique entails applying high-energy microwave radiation to initiate standard chemical reactions by breaking up chemical bonds and creating the CQDs owing to the microwave's ability to heat all chemical samples uniformly [40]. Microwave synthesis is a rapid and fairly economical method of synthesising CQDs by microwave heating, as depicted in Figure 3. The process is quite simple and economical in terms of time since it improves the quantum yield of CQDs relative to the other methods [41]. Different studies reported the synthesis of CQDs by this method. An efficient and controlled synthetic approach of carbon dots has been reported using branched polyethyleneimine and citric acid, which were employed to change the internal structure [42]. Such a system supports the versatility of carbon dots that could be developed easily by facile fabrication methods, combining catalytic properties and photoluminescence. Nazar, Muhammad, et al. synthesised CQDs via a pot microwave-assisted heating method from activated carbon of arabica coffee waste with a size of 10.12 nm and a quantum yield of 6%, performing as a selective fluorescent detector for $Fe^{3+}$ ions, with a detection limit of 0.27 µM [43]. Architha, Natarajan, et al. synthesised CQDs from the Plectranthus amboinicus (Mexican Mint) leaves via the microwave-assisted reflux method with a QY of 17% and an average diameter of 2.43 nm and used a fluorescent probe for $Fe^{3+}$ ion detection with LOD of 0.53 µM in the concentration range of 0–15 µM. CQDs prepared showed excellent properties in terms of detection of $Fe^{3+}$ ions and biological applications [44]. Chugh, Riya, and Gurmeet Kaur, et al. successfully prepared CQDs-Ag NCs with the average sizes of orange peels mediated CQDs around 5–8 nm, which showed great potential in precision agriculture and bactericidal applications [45]. Zaman, Alif Syafiq Kamarol, et al. successfully synthesised CQDs from empty fruit bunch EFB biochar for the sensitive and selective detection of $Cu^{2+}$ ions, which showed a concentration range of 0–400 µM, acting as a fluorescent sensor [46].

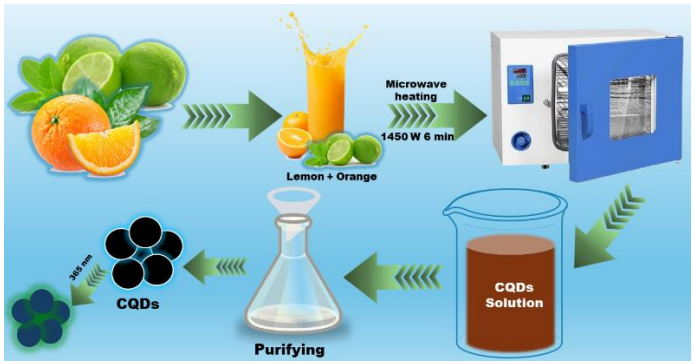


**Figure 3:** *Biomass-Derived Highly Luminescent CQDs via Hydrothermal Carbonisation of Lemon [47]*

### 3.3. Microwave Assisted Synthesis

The carbonisation method of CQD synthesis uses organic precursors such as glucose or citric acid and heats the precursors at temperatures between 200 °C and 900 °C in an inert or low-oxygen atmosphere. This process includes the thermal decomposition of carbon precursors to produce carbon nanoparticles of definite characteristics based on the temperature, time, and type of precursor, as illustrated in Figure 4. This cheap technique can easily control the size of the CQDs for uses in bioimaging, sensing, and optoelectronics. Suppan, Thangamani, Rama Ranjan Bhattacharjee, and Moorthi Pichumani. prepared Fluorescent 'turn-on' porphyrin CQD nanoprobes for selective sensing of heavy metal ions. Porp-CQDs have an average particle size of 2.4 nm and sensed the $Zn^{2+}$ ions in bore well water analysis with LOD of 75 µM [48]. Kaur, Rajdeep, et al. reported the synthesis of (AgNPs-CQDs) nanocomposite from *Syzygium cumini* leaves by pyrolysis treatment with an average diameter of 4.0 nm for $Hg^{2+}$ ions detection, which was demonstrated as an outstanding colourimetric sensor for mercury detection over wide PH ranges [49]. Kumari, Archana, et al. prepared green fluorescent CQDs waste polyolefins residue for $Cu^{2+}$ ion in real water samples, having QY of 4.84% with LOD value of 6.33 nM and linear detection range of 1–8.0 M. Prepared CQDs also showed potential for cancer cell imaging [50].

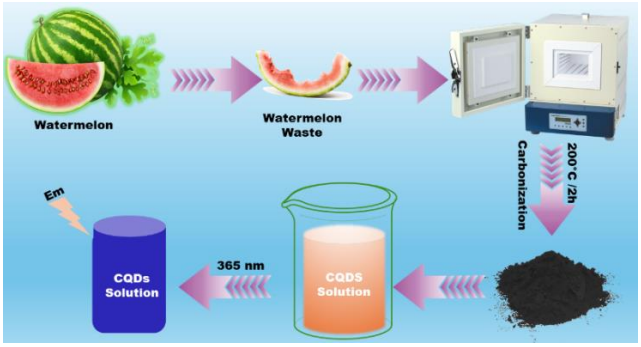


**Figure 4**: *Schematic illustration of the synthesis of water-soluble fluorescent CQDs from watermelon peels [51]*

## 4. Comparison of synthesis methods of CQDs

Several techniques are used to prepare Carbon Quantum Dots, and each technique comes with advantages and disadvantages depending on the application of CQDs. The top-down methods include laser ablation and electrochemical oxidation, while the bottom-up methods include hydrothermal/solvothermal, microwave-assisted, and pyrolytic synthesis [22]. Top-down techniques can be achieved by breaking down larger carbon structures into smaller units, typically highly crystalline CQDs. Nevertheless, these methods may be energy-consuming and imply the usage of highly specialised equipment [52]. On the other hand, the bottom-up approach builds up the CQDs from molecular precursors and they provide more control over the size and surface characteristics of the dots [21],[22]. Of the above methods, it is hydrothermal to convert the organic materials into CQDs, where water acts as a solvent under high temperature and pressure. This method is widely appreciated due to its benefits, such as simplicity in the synthesis process, being cheaper as compared to other techniques, and the ability to synthesize CQDs with desirable optical characteristics. Microwave-assisted synthesis, another bottom-up approach, significantly reduces the reaction time by providing heat evenly and rapidly, although the particle size distribution may not always be uniform [53]. Pyrolysis is another common technique characterized by a high yield of CQDs but its reaction conditions might be more demanding and critical for getting uniform and high quality of CQDs. Thus, the type of synthesis of the CQDs depends on the purpose, required characteristics, costs, and environmental friendliness of the method, as each offers a trade-off between accuracy and yield [54] (Table 2).

**Table 2**
Comparative Analysis of Synthesis Methods of CQDs.

| Synthetic Methods | Advantages | Disadvantages | Ref. |
|---|---|---|---|
| Chemical Ablation | Highly efficient, Most Accessible Surface functionalization | Hazardous byproducts, Requires careful handling Poor control over size | [55] |
| Electrochemical Carbonization | stable and one-step method, mild conditions | High energy consumption, complex setup | [56] |
| Laser Ablation | Precise control over the size, rapid, tunable surface states | Complex laser system, Low Quantum yield | [56] |
| Hydrothermal Treatment | Eco-friendly, economical, non-toxic, easy procedure | Poor control over size, Risk of explosions | [57] |
| Microwave Assisted | Cost-effective, rapid, and desired morphology can be obtained | poor control over size, | [57] |
| Pyrolysis | Produce good products High yield, thermal stability | Controlled atmosphere, High-temperature requirement | [58] |

### 4.1. Microwave Assisted Synthesis

CQDs are formed by sheets of graphene or derivate graphite. These dots have a high surface area-volume ratio as well as $sp^2$ hybridisation of the crystalline core and non-crystalline phases with surface functional groups [59],[60],[61],[62]. Tang et al. discovered that carbon quantum dots (CQDs) have core-shell structures, which can be either amorphous (mixed $sp^2/sp^3$) or graphitic crystalline ($sp^2$), depending on the extent of $sp^2$ carbon occurrence in the core [63]. Several researchers reported the graphitic crystalline core of CQDs, as can be seen in Figure 5 [64],[65]. The cores are classified based on the synthesis technique, precursors, and other parameters [66]. These cores are very small, ranging from 2-3 nm with a lattice spacing of ~0.2 nm [67]. At temperatures above 300°C, the structure becomes graphite-like ($sp^2$), while lower temperatures result in amorphous cores unless there is a presence of $sp^2/sp^3$-hybridised carbon in the precursor [68]. To determine the core structure of CQDs, various instrumental techniques such as Transmission Electron Microscopy (TEM) or High Resolution (HR) TEM, Scanning Electron Microscopy (SEM), Raman spectroscopy, and X-ray diffraction (XRD) are utilised. TEM and SEM (FESEM) are usually carried out to measure CQDs' size and morphology [69]. SAED and XRD patterns reveal the crystalline or amorphous nature of CQDs. The same selected area electron diffraction (SAED) pattern is observed for CQDs passivated by polyethylene glycol (PEG200N) via laser ablation, which corresponds to the planes of the diamond structure [70]. The HRTEM image reveals varying lattice spacing ranging from 0.2-0.23 nm. The wide peak at 2θ 23° suggests that the CQD has an amorphous characteristic, whereas the presence of two wide peaks at 2θ 25° and 44° indicates a low-graphitic carbon structure similar to (002) and (100) diffraction [71]. The composition and functional groups on the surface of CQDs are analyzed using techniques such as FT-IR spectroscopy, XPS and NMR [7].

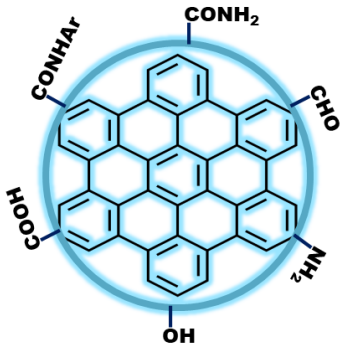


**Figure 5**: *Structure of CQDs*

Recent research has focused on studying fluorescent carbon quantum dots (CQDs) for multi-ion sensing and bio-imaging applications. Arumugham, Thanigaivelan, et al. discovered that CQDs derived from Catharanthus roseus leaves demonstrated carboxylic functional groups on their surface and contained major exciting elements such as carbon (C, wt. 98.14%), oxygen (O, wt. 0.73%), and nitrogen (N, wt. 1.13%) from the EDX spectrum as support for the FT-IR result [72].

The zeta potential is used to determine the positive or negative charge on the surface of CQDs and the level of electrostatic interaction between them [73]. Kolanowska, Anna, et al found that Lys- and Cys-CQDs had the highest zeta potential values, providing excellent stability in water [74]. In highly acidic conditions, most amine groups were protonated, resulting in an overall higher positive surface charge. Conversely, in alkaline conditions, the zeta potential remained highly negative, indicating the presence of stable anions for all CQDs.

## 5. Properties of CQDs

Carbon quantum dots exhibit diverse and tunable physicochemical properties that make them highly attractive for advanced technological applications. Their behaviour is strongly influenced by size, surface functional groups, doping elements, and synthesis conditions. This section discusses the fundamental optical, photoluminescence, and electronic properties of CQDs along with their characterisation aspects.

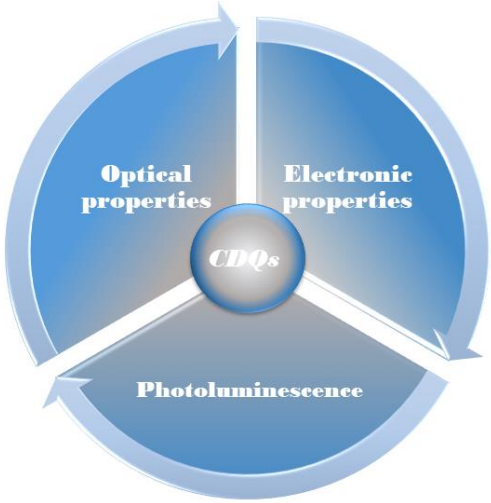


**Figure 6**: *Properties of CQDs*

### 5.1. Optical Properties

Carbon quantum dots have unique optical characteristics, making them very useful in sensing, imaging, and photonics applications. Out of all the varieties of CQDs, they exhibit high and size-tunable photoluminescence, where the size, the type of surface groups, and the synthesised conditions could help in adjusting the luminescence properties [75]. Carbon dots commonly demonstrate significant absorption in the ultraviolet range (230-400 nm), with some absorption bands extending into the visible spectrum [76]. The π-π* transition of the C=C bond produces the distinctive peak at 260-320 nm, while the n-π* transition of the C=O bond accounts for the shoulder peak at 270-390 nm [77]. Modifying the surface through passivation or functionalization can alter the UV absorption properties of carbon dots by enhancing their absorption peaks or shifting their absorption wavelengths towards the red end of the spectrum, referred to as quantum confinement [78].

Quantum yield and fluorescence intensity in carbon quantum dots (CQDs) are linked, with intensity increasing as quantum yield rises. Surface passivation [79] and doping [80] are key factors influencing quantum yield. Additionally, fluorescence is affected by particle size, pH level, and surface functional groups [81]. Surface passivation using 1-ethyl-3-(3-dimethyl aminopropyl)-carbodiimide (EDC) can significantly increase the fluorescence intensity of CQDs. The fluorescence intensity increases with the amount of EDC, reaching a maximum at 25 mM concentration, with the quantum yield increasing from 18.83% to 41.10% [82]. Highly passivated green phosphorus-nitrogen co-doped CQDs with a 25% quantum yield were prepared by Omer. CQDs can detect $Cu^{2+}$ ions at concentrations as low as 1.5 nM [83]. Wang synthesised CQDs with a 53% quantum yield using a solvothermal method. Using citric acid as a precursor and 1-hexadecylamine as a surface passivator [84]. Inorganic salts such as ZnS and $TiO_2$ can be used to dope carbon quantum dots (CQDs) to enhance fluorescence quantum yield along with surface passivation [85]. Anilkumar successfully raised the quantum yield of CQDs doped with inorganic salts and surface passivation, with ZnS-doped CQDs reaching a 78% quantum yield and TiO2-doped CQDs achieving a 70% quantum yield [86]. Additionally, nitrogen/sulfur co-doped CQDs were produced with a quantum yield of up to 73.1% using citric acid and thiourea as reaction precursors in a hydrothermal approach. These CQDs could be used as fluorescent probes for detecting uric acid [87].

Various methods of creating doped carbon quantum dots (CQDs) have been explored in recent studies. Bourlinos utilised microwave heating to produce nitrogen/boron co-doped green fluorescent CQDs using citric acid, boric acid, and urea as a source [88], while Zhou employed the solvothermal approach to create phosphorus-doped CQDs with a 25% fluorescence quantum yield hydroquinone and phosphorus tribromide as a carbon and phosphorus source [89]. These findings indicate that doping CQDs with specific electron groups and heteroatoms can significantly alter their luminescence properties, making them particularly valuable for various applications.

In synthesising CQDs, adjusting the synthesis conditions can alter their physical and chemical properties, such as particle size and surface chemical composition, affecting their energy level structure and photochemical properties [90]. By modifying the concentration of alkali [90] and using oxidising or reducing reagents during synthesis, the chemical composition of the surface can be adjusted, leading to changes in the photochemical properties of CQDs [91].

Carbon quantum dots have high light absorption capability and can extract light at difficult and complex wavelength ranges. This characteristic is most useful for applications in solar cells and photocatalysis since there is a need for the material to absorb light of many wavelengths [92]. For instance, surface passivation can enhance the fluorescence quantum yield and stability greatly. However, it is possible to modify these properties with simple and cost-effective synthesis approaches of CQDs, thus making them applicable in the progression of the bioimaging, optical sensing, and energy conversion science fields [17].

### 5.2. Photoluminescence

Research on the photoluminescence (PL) of CQDs) has experienced significant growth in recent years. This property has been particularly valuable in the field of photocatalysis [93]. The PL emission of CQDs follows the Stokes type emission, meaning that the emitted wavelength is longer than the excitation wavelength; several literatures reported this [94],[95]. In the analysis of emissions and structural features, most observed PL emissions can be categorised into bandgap transitions related to p-domains and origins associated with defects in graphene structures. These categories are often interconnected as the creation of p-domains is based on the manipulation of defects in graphene sheets [96]. In a plethora of studies, the correlation between PL emission and excitation wavelength (λex) of CQDs has been extensively discussed. Sun et al. noted that fluorescent CQDs, modified with polyethylene glycol (PEG1500N) or propionyl ethyleneimine co-ethyleneimine (PPEI-EI), exhibit distinct emission patterns based on the excitation wavelength [97].

Carbon quantum dots were synthesised hydrothermally by Ding et al., using urea and then separated via silica column chromatography. The CQDs exhibited a single peak in the photoluminescence excitation spectrum and the excitation-independent PL emission spectrum. Additionally, they displayed similar monoexponential fluorescence lifetimes. The absorption curves and PL emission spectra under different light wavelengths are depicted in Figure 6.

In the latter case, it was found that the fluorescence change in CQDs) is mainly influenced by surface functional groups [98], which create energy potential traps mostly led by sp2 and sp3 hybridised regions [99]. The defect-derived fluorescence of doped

CQDs is attributed to the localised electron structure of electron-hole pairs in the $sp^2$ state, and the fluorescence quantum yield can be significantly increased through doping [100]. It was also discovered that modifications to surface groups have a significant effect on the fluorescence emission of CQDs [101]. This indicates the potential for enhancing the optical properties of CQDs through surface group modifications.

Fang, Li-yang, and Jing-tang Zheng. Conducted a study using hydrothermal synthesis to produce C-dots-160 and C-dots-200 at temperatures of 160°C and 200°C. The research aimed to understand the relationship between microstructure and fluorescence emission behaviour of CQD-dots. It was found that higher synthesis temperatures led to the addition of more oxygen and nitrogen atoms, increasing structural flaws and altering their concentration ratio. Consequently, C-dots-200 exhibited stronger fluorescence emission [102].

Certain carbon dots possess up-conversion photoluminescence characteristics [103],[104] which involves the release of light with a shorter wavelength after absorbing two or more photons with a longer wavelength. This process is characterised by the emission of light at a higher energy than the absorbed photons [105]. Cao et al. demonstrated in their study that CQDs) produced through laser ablation exhibit strong luminescence with two-photon excitation in the near-infrared at 800 nm, suggesting the presence of up-conversion photoluminescence (UCPL) properties [103].

### 5.3. Electronic Properties

The synthesised CQDs) possess remarkable electrochemical features that qualify them to be used in sophisticated technologies, for instance, optoelectronic [106],[107], and energy storage technologies [108],[109] among others. The first of the most prominent electronic features of CQDs is their size and shape-tunable bandgap. This tunable bandgap also helps CQDs to enable them to extend from the intrinsic characteristic of bulk carbon materials to act like other regular semiconductor CQDs for use in electronic and photonic applications [110],[111]. Also, CQDs possess high electron mobility, which is desirable in the application of the material in electronic circuits and devices. This high electron mobility is attributed to the $sp^2$ hybridised carbon networks carved in the CQDs, which offer efficient paths for electron transport [112]. Carbon Quantum Dots CQD in the electron transport layer with $TiO_2$ accelerate the efficiency of perovskite solar cells by up to 19%. This enhancement is because CQDs offer higher electron mobility and decreased charge recombination compared to the control. This CQDs/$TiO_2$ composite also allows for achieving greater stability and reproducibility of cells. This approach shows that the CQDs can enhance the performance of the photovoltaic devices [113]. Besides, CQDs demonstrated specific features of charge accumulation, which could be quite appealing for application in supercapacitors [114] as well as batteries [115]. Due to a large surface area to volume ratio and high electrode materials' rate capability, it is possible to charge them to store energy and quickly discharge [116]. Surface functionalization of CQDs can increase their electronic characteristics by appending appropriate functional groups that will increase conductivity and interface compatibility with other materials. For example, when nitrogen or sulfur is doped into CQDs, it will cause a great change in their electronic structure concerning the effect of enhanced charge transfer and electrical conductivity [114]. The electronic properties' multiple and tunable nature and their synthesis method's simplicity and eco-friendly nature make CQDs an ideal candidate to bring about the next generation of electronic, optoelectronic, and energy storage devices [117].

## 6. Methods used for characterisation of CQDs

To describe CQDs, many techniques are used for characterising as well as examining the properties of Carbon Quantum Dots. With the help of TEM, SEM, XRD, and AFM characteristics of structural properties, including the size of particles and the surface morphology and crystalline structure, are observed. In properties of light interaction, UV-Vis spectroscopy (200–800 nm) is used to understand absorption and PL Spectroscopy (200–1000 nm) for fluorescence and decay.

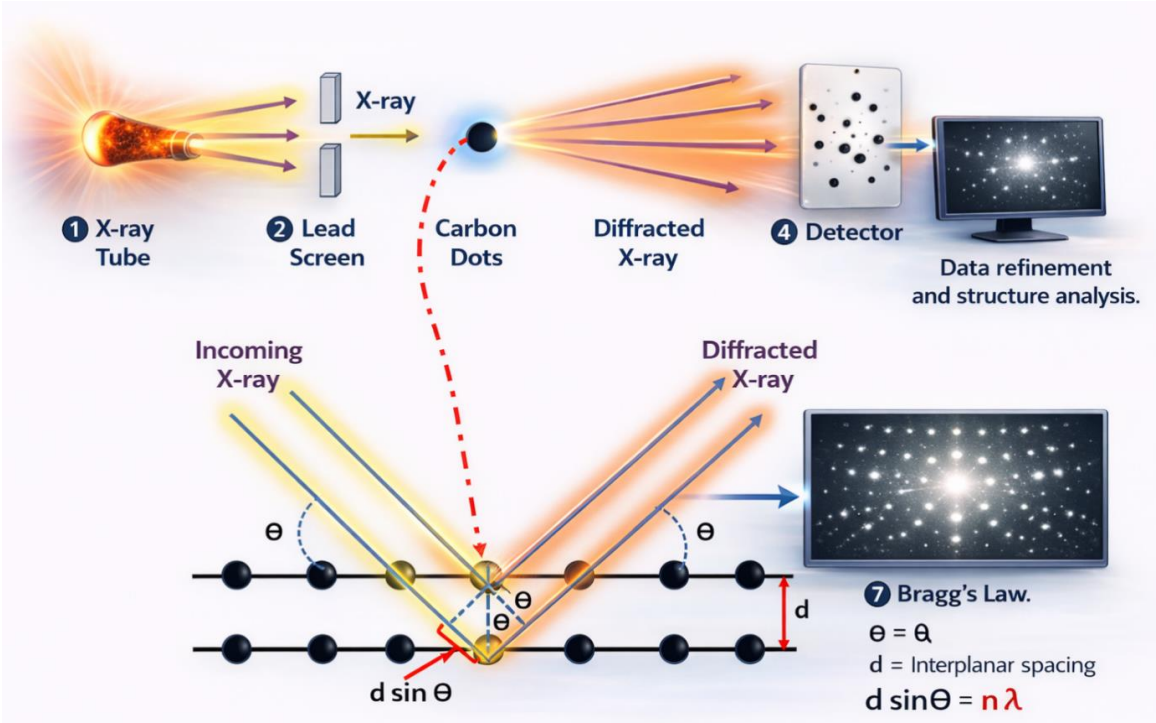


**Figure 7**: *Schematic representation of X-ray diffraction showing the interlayer spacing (d) and the incident/diffracted angle (θ) of X-rays according to Bragg's law*

Functional groups and components are determined with FTIR, XPS, Raman, and EDX. Zeta Potential Measurement and DLS are used to analyse and measure surface characteristics of the charge and stability, respectively. DSC is complemented by TGA and NMR Spectroscopy for further information on thermal stability and information about the molecular structure [118].

### 6.1. Morphological Analysis using TEM/ SEM

The utilisation of scanning electron microscopy (SEM) and transmission electron microscopy (TEM) in CD visualisation is widely acknowledged by researchers. In the comparison between SEM and TEM for imaging CQDs, SEM uses a focused electron beam to scan the surface and obtain information on surface topography and composition, while TEM is more precise for measurements smaller than 1–20 nm due to its higher resolving power, making it better for identifying small-sized particles [119]. TEM utilises high-energy electron beams to transmit through the sample for imaging. TEM has been used to investigate the morphological evaluation of CQDs, including their nanostructure and size down to the quantum scale, with an average size of 2-12 nm [120],[121],[122]. Based on a recent report, CQDs showed nearly spherical and uniformly sized particle indicating the crystalline nature of the prepared CQDs [69]. The inter-layer spacing and average crystallite size of CQDs were found to be around ~1.8 Å and 1.9 nm, respectively. Cheng et al. used the HRTEM technique to identify that the average size of CDs was 3.4 nm. Their HRTEM images revealed that the CD particles appeared in quasi-zero dimension and were highly crystalline, with a size distribution ranging from 1 to 10 nm [123]. The carbon nanostructures displayed uniform particle size distribution and minimal aggregation, with an average diameter of 7.89 nm based on the Gaussian fitting curve. This was determined by measuring around 200 particles, indicating nano-sized characteristics. In another report, the study analyzed the size distribution of C-CQDs from TEM images, finding sizes ranging from 2-12 nm with an average size of 5 nm. The C-CQD structure exhibited crystallites on the surface/edge and in the core, indicating mixed-phase growth [124]. The average size of 18-20 nm CQDs was identified by Baslak, Canan, et al. via the HRTEM technique. HR-TEM showed that the shape of the synthesised CQDs was almost quasi-spherical, with an essentially amorphous core structure and no crystal lattice. DLS analysis also confirmed the TEM images [125].

### 6.2. Structural Analysis using XRD

Regarding the structural characterisation of CQDs, X-ray diffraction (XRD) is a vital method. It allows us to determine whether the CQDs are crystalline and to analyze their phase composition. The diffraction patterns provide information about interlayer spacing, crystallite size, and the level of graphitisation as depicted in Figure 7 [110]. Typically, the diffraction band at 2θ = 20–30° is attributed to the amorphous structure of CQDs, while sharp bands indicate crystalline clusters [111],[112]. In a study by Singh, Arvind, et al., self-functionalized luminescent CQDs were prepared through nanosecond laser irradiation. XRD analysis showed that these CQDs exhibited weaker, broader diffraction peaks at around 22.5°, with a d-spacing of approximately 0.4 nm, compared to the (002) plane of highly crystalline graphitic microcrystals at about 26.5° with a d-spacing of roughly 0.35 nm. This suggests a polycrystalline nature, likely caused by oxygenated groups. The peak width increased as the particle size decreased [112]. Fluorescent CQDs were also produced from sugarcane bagasse pulp using a chemical oxidation and exfoliation process. The XRD analysis identified characteristic peaks at 2θ = 11.4°, 20.6°, 22.8°, 42.3°, and 45.7°, with prominent peaks at 20.6° and 42.3°, indicating the presence of graphitic carbon. Additionally, SAED patterns and XRD peaks confirmed that the CQDs possess a face-centred cubic crystal structure matching carbon's diffraction pattern. The observed interlayer spacing aligns with the (311) plane of carbon [113].

The Debye-Scherrer formula was used to calculate the average grain size of prepared CQDs by selecting the highest peak value shown in the XRD diffractogram (1).

$$D = \frac{K\lambda}{\beta \cos\theta} \quad (1)$$

In the previously mentioned equation, $\boldsymbol{D}$, $\boldsymbol{K}$, $\boldsymbol{\theta}$, $\boldsymbol{\beta}$ and $\boldsymbol{\lambda}$ represent the dimensions of the carbon quantum dot, k refers to the constant shape factor within the range of 0.89–1, with a value of 0.9 in this particular study [126], the measured diffraction Bragg angle in degrees, β is the full width at half maximum denoted as FWHM and measured in radians, and λ is the wavelength of the X-ray source, which is 0.15406 nm (Cu$k_{\propto}$ radiation), respectively. By utilising the equation, the average grain size of the prepared quantum dots was 2 nm and 4 nm.

XRD is crucial for identifying the key characteristics of crystallite-structured C-dots, but it is not suitable for analysing amorphous C-dots. Such structural information is important for understanding the electronic properties of CQDs in fluorescence sensing and photocatalytic fields.

### 6.3. Morphological Analysis using AFM

Innovative tools like Atomic force microscopy (AFM) are useful in the characterisation of Carbon Quantum Dots and help in the determination of surface morphology and topographical features. AFM offers very accurate measurements of the size, height, and lateral dimensions of CQD particles, which are important when determining the distribution of the sizes of these particles as well as the roughness of the surface. In the same vein, AFM determines the aggregation state of the CQDs and evaluates stiffness as well as adhesion coefficients of the material at the nanoscale. This characterisation provides a detailed, comprehensive profile of CQDs that will enable researchers to enhance fluorescence sensing and photocatalysis applications of CQDs with the best understanding and performance.

AFM works on a setup where a fine tip is placed at a very close distance from the sample material in the form of a flexible lever. The idea of AFM relies on force interactions between the tip and the sample or the surface of the specimen [127]. When the tip scans along the surface, forces such as the van der Waals force the cantilever to bend. A laser beam is reflected off the cantilever, which records these deflections using a photodetector. The collected data is then analysed to produce full-scale, three-dimensional representations of the sample surface [128]. This method enables AFM to offer topographical information and other physical properties at a nanoscale, which makes it productive for characterising nanomaterials such as CQDs. The research used AFM images to measure the size and roughness of the synthesised CQDs. The CQDs were observed to be spherical and very small, with average diameters ranging from 3 to 5 nm and surface roughness of less than 5 nm [129]. The images in Figure 4 illustrate the random arrangement of the CQDs on a silicon wafer substrate at low magnification and provide high magnification images as well as a 3D image with corresponding 2D images. The histogram of the CQDs indicated an average roughness of 4.2 nm and a size ranging from 3 to 5 nm [129].

### 6.4. Optical Analysis using UV/Vis Spectroscopy

The optical absorption of carbon quantum dots (CQDs) is excellent in the 260 to 320 nm UV range, extending into the visible

region. Pure CQDs typically show two absorption peaks, one for the π-π* transition of aromatic $sp^2$ domains and one for the n-π* transition of surface functional moieties like carbonyl, hydroxyl, ester, and carboxyl groups [94]. However, the position of these peaks heavily relies on the CQDs' synthetic method and the nature of their surface groups [130]. General instrumentation of Uv-Vis spectroscopy is shown in Figure 8.

The optical properties of CQDs are significantly affected by their size, shape, and surface functionalization, leading to shifts in absorption peaks as the size decreases. Additionally, surface functional groups can impact the electronic structure, altering the absorption characteristics. UV–visible spectroscopy is crucial in determining the optical bandgap of CQDs, which is essential for assessing their potential applications in optoelectronic devices [131].

UV-visible spectroscopy is crucial for determining the bandgap of CQDs, which indicates their semiconducting nature and suitability for electronic applications. The absorption spectra provide insights into the behaviour of CQDs under different conditions by indicating variations in size, aggregation, or surface chemistry. The bandgap energy can be precisely determined through meticulous preparation and analysis, enabling a systematic procedure. The construction of a Tauc plot aids in enhancing precision for this purpose [132]. The plot shows a relationship between $(\alpha h\nu)^2$ and photon energy (hν), with α representing the absorption coefficient and hν denoting photon energy. The bandgap energy can be determined by identifying where the tangent line intersects the energy axis at the steepest part of the curve. Subsequently, the bandgap energy can be calculated using a specific equation [133].

$$Eg = hc/\lambda \qquad (2)$$

***Eg*** denotes the bandgap energy, ***h*** signifies Planck's constant, ***c*** epitomises the speed of light and ***λ*** represents the wavelength corresponding to the absorption edge. Bano et. al synthesized photoluminescent N-CDs from Tamarindus indica leaves using the hydrothermal method at 210 °C. When exposed to UV light at 365 nm in a UV chamber, these N-CDs emitted a blue colour. A single absorption peak at 280 nm was observed, attributed to the π-π* electronic transition of the C=C bond [134]. Vaibhav Naik et al. discovered that nitrogen-doped carbon dots, synthesised using a hydrothermal method and ammonia, have potential applications in detecting dopamine and multicolour cell imaging. Their UV-VIS spectroscopy analysis revealed a peak at 278 nm (π-π*), indicating the presence of aromatic $sp^2$ domains. Furthermore, the addition of dopamine led to a red shift in absorption maxima, suggesting the formation of a ground-state complex between the carbon dots and dopamine [135].

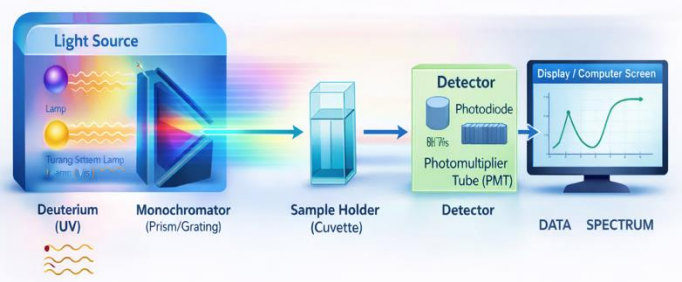


**Figure 8**: *A schematic representation of the setup employed for recording UV–visible absorption spectra*

### 6.5. Fourier Transform Infrared Spectroscopy

Fourier transform infrared (FTIR) spectroscopy is a widely employed technique to identify surface functional groups present on carbon quantum dots (CQDs) and to confirm successful surface passivation. A schematic overview of the general instrumentation is presented in Figure 9. The FTIR spectra of CQDs typically display a broad absorption band in the range of 3200–3500 $cm^{-1}$, which is attributed to the stretching vibrations of hydroxyl (–OH) and amine (–NH) groups, often arising from surface-bound functional moieties and adsorbed moisture [136],[137]. The appearance of absorption bands near 2900 $cm^{-1}$ is generally associated with C–H stretching vibrations, indicating the presence of aliphatic carbon structures on the CQD surface [138]. Distinct peaks observed around 1700–1650 $cm^{-1}$ correspond to the stretching vibrations of carbonyl (C=O) groups, confirming the presence of carboxylic functionalities formed during oxidative carbonisation processes [139]. Additionally, absorption bands in the region of 1600–1550 $cm^{-1}$ are commonly assigned to C=C stretching of aromatic or graphitic domains and N–H bending vibrations, suggesting partial graphitisation and nitrogen incorporation within the CQD framework [3]. The presence of C–O stretching vibrations is evidenced by peaks appearing between 1200 and 1100 $cm^{-1}$, which are indicative of hydroxyl, ether, or epoxy groups (C–O–C) on the CQD surface [65]. Lower wavenumber peaks in the range of 800–900 $cm^{-1}$ are typically attributed to C–H bending or out-of-plane vibrations of aromatic rings [138].

The abundance of oxygen- and nitrogen-containing functional groups revealed by FTIR analysis highlights the hydrophilic nature and excellent aqueous dispersibility of CQDs, which are crucial for their fluorescence behaviour and metal ion sensing performance [9]. While FTIR provides valuable insight into surface chemistry and functional group distribution, it offers limited information regarding the detailed core structure or heteroatom coordination within CQDs. Therefore, FTIR analysis is often complemented with other characterisation techniques for comprehensive structural evaluation [138].

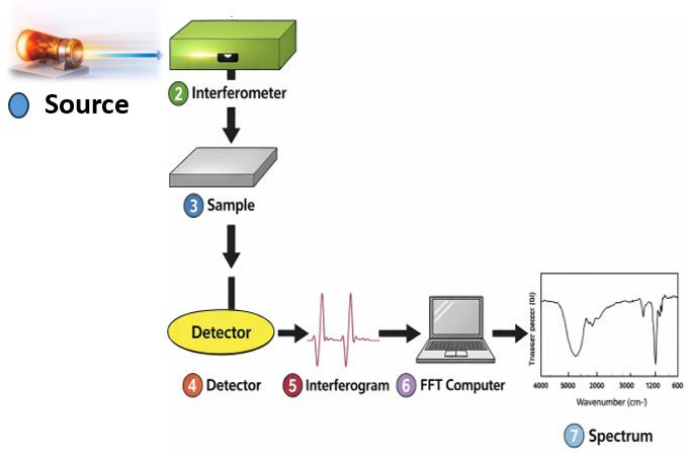


**Figure 9**: *Diagram representing the basic configuration employed for FTIR measurements*

## 7. Fluorescence-Based Sensing Applications of Carbon Quantum Dots

One of the most distinctive advantages of CQDs is the ability to tailor their fluorescence characteristics through controlled synthesis and surface engineering. Particle size, degree of graphitisation, surface oxidation, and heteroatom incorporation directly influence band gap energies and emission wavelengths. Smaller CQDs generally exhibit blue-shifted emission due to stronger confinement effects, whereas larger or surface-modified CQDs often display red-shifted fluorescence [140]. This tunability, combined with broad excitation spectra and narrow emission bands, makes CQDs versatile fluorescent probes for sensing applications.

Figure 10 illustrates the schematic representation of the photoinduced electron transfer (PET) process governing the fluorescence quenching behaviour.

The carbon quantum dots in fluorescence modulation are based on the special interactions of the excited states of CQDs with the analytes, and the mechanism predominantly depends on the electronic band of CQDs and the optical or chemical properties of the target. The Static quenching It is possible that the radiative recombination is inhibited by forming stable ground-state solutions with the surface functional groups (e.g., carboxyl, amine, or thiol) by the heavy metal ions on CQDs, and thereby avoiding radiative recombination without affecting the fluorescence lifetime significantly, as was shown in $Fe^{3+}$ sensors where the complexation alters the absorption character but preserves the decay kinetics. More fundamentally, dynamic quenching is significant when the excited CQD and the analyte have spectral overlap, with a preference for FRET under conditions of proximity and strong coupling between the two dipole charges, where the former electronically transfers energy to the electron donor and the latter electronically transfers energy to the electron acceptor [141]. In contrast, IFE is observed when the redox potential of the analyte is no longer favourable. The excited CQD undergoes direct absorption or emission of the excitation light or emission light by the quencher without energy transfer, as has been demonstrated systematically in the graphene quantum dots under different pH conditions [142]. Photoinduced electron transfer (PET): This occurs when the redox potential of the analyte matches that of the excited CQD, which is frequently the cause of such strong quenching to electron-deficient ions as $Fe^{3+}$ or $Cr^{6+}$ [143]. A recent study has shown that solvent-sensitive surface activity in N, S-doped CQDs can directly determine the dominance of static- or dynamic-quenching pathways, reflecting the role of surface chemistry in tuning mechanism and sensitivity. Notably, these processes do not work alone; in most real-world sensing systems, IFE, PET, and FRET synergetically interact, and in order to isolate each mechanism, lifetime measurements and spectral analysis of a combination are necessary to determine which process is selective to a given heavy metal ion [144].

In fluorescence-based sensing, CQDs function as signal transducers whose emission intensity, wavelength, or lifetime changes in response to interactions with target analytes. These interactions may occur through adsorption, coordination bonding, electrostatic attraction, or redox reactions at the CQD surface [145]. Quantitative analysis is commonly achieved by establishing a linear relationship between fluorescence response and analyte concentration, allowing CQDs to serve as sensitive and reproducible sensing platforms [146].

Surface functionalization plays a crucial role in determining the selectivity of CQD-based sensors. The abundance of oxygen- and nitrogen-containing functional groups such as carboxyl, hydroxyl, amino, and amide moieties on CQD surfaces enables strong interactions with specific target species [147]. By modifying surface chemistry or introducing selective ligands, CQDs can be engineered to preferentially recognise and bind particular analytes, including metal ions, small molecules, and biomacromolecules [7].

Fluorescence modulation in CQDs may arise from several mechanisms, among which fluorescence quenching is most commonly exploited for sensing. Förster resonance energy transfer (FRET) has been widely applied in CQD-based sensors, where CQDs act as fluorescent donors and transfer energy to suitable acceptors in a distance-dependent manner [148]. Effective FRET requires spectral overlap between CQD emission and acceptor absorption, as well as donor–acceptor separation typically within 5–10 nm. The broad absorption range and tunable emission of CQDs allow precise control over such spectral overlaps, making them excellent candidates for FRET-based sensing systems [149].

These features of structure determine the dominance of the quenching pathway when metal ions are added. As an example, weakly bound surface ligands, including -COOH, -OH, and $-NH_2$, can bind strongly with the cations, forming efficient photoinduced electron transfer (PET) between the excited CQDs and the metal centre, resulting in fluorescence suppression [150]. Where there is spectral overlap between the CQD emission and the absorption band of the analyte, the FRET or inner filter effects can be realised.

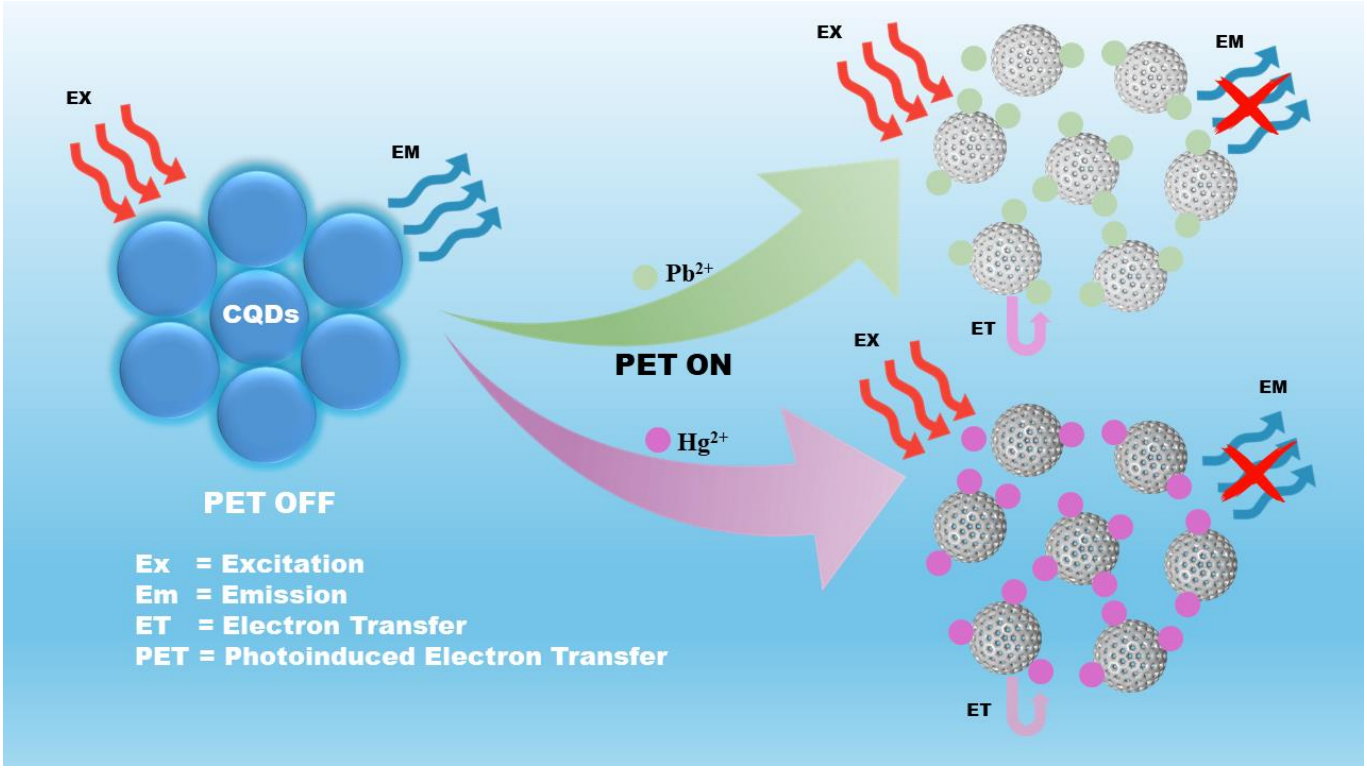


**Figure 10**: *PET Quenching Mechanism*

In the meantime, strongly defective surfaces might encourage the small-scale structure formation, and more weakly interacting interfaces might encourage dynamic collisional quenching [151].

Notably, sensing selectivity derives from preferential binding affinities when the oriented surface functionalities are compared to the particular ionic radii or redox potentials. As an illustration, sulfur- or nitrogen-bearing locations can tend to increase the recognition of softer acids like $Hg^{2+}$, whereas oxygen groups can prefer a more rigid metal ion. This leads to the logical approach of tuning electron-transfer probability by careful control of passivation, doping, and surface charge to achieve enhanced analytical discrimination [152].

In addition to FRET, fluorescence responses in CQDs can be influenced by the inner filter effect (IFE), static quenching, and dynamic quenching. IFE occurs when absorbing species in the system attenuate the excitation or emission light, leading to reduced fluorescence intensity without affecting fluorescence lifetime. Static quenching is when the fluorophore (e.g., CQDs) reacts with the quencher to form a non-fluorescent complex, usually with heavy metal ions [153],[154],[155]. This occurs before the fluorophore is exposed to light in a process that prevents fluorescence emission. The quenching depends upon the formation of a stable complex and is generally characterized to have a different temperature and concentration-dependent behaviour from the other mechanisms [156]. Li, Zhaofa, et al. synthesised a hybrid nanoprobe composed of N-doped CQDs and L-cysteine-capped CdSe/ZnS QDs combined with $Cu^{2+}$ to form a stable complex, leading to the static quenching of L-cysteine-capped CdSe/ZnS QDs [157].

Whereas dynamic quenching results from collisional interactions in the excited state. In dynamic quenching, the quencher molecule gets to the vicinity of the fluorophore after the

**Table 3**
Recent green CQDs produced by the Bottom-Up approach

| Source | Target | Readout | Synthesis method | QY (%) | Detection limit | Average Size & Color | Ref |
|---|---|---|---|---|---|---|---|
| **Mango leaves** | $Fe^{2+}$ | Fluorescent | Pyrolysis 300 °C for 3 hrs | ~18.2% | 0.62 ppm | Blue 1–5 nm | [162] |
| **Cabbage** | $Fe^{3+}$ | Fluorescent | Hydrothermal 140 °C for 5 h | | 1.72 x 10−7M | 2–4 nm | [35] |
| **CQDs/ZnO/CdS NPs** | $Fe^{3+}$ | Fluorescence | Hydrothermal 200 °C for 5 h | | 1.72 × 10−7 M | | [36] |
| **banana juice** | $Cu^{2+}$ | Fluorescent | hydrothermal 150 °C for 4 h | 32 % | 0.3 µg mL−1 | Blue 1.27 nm | [163] |
| **biomass tar** | $Cu^{2+}$ | Fluorescent | reduction smelting process | 27.3% | 80 nmol/L | 1.98 nm | [164] |
| **Poplar wood powders** | $Cr^{3+}$ | Fluorescence | hydrothermal 180 °C for 8 h | | | Blue-Green 6-8nm | [165] |
| **CQD@γ-Fe2O3** | $Hg^{2+}$ | Fluorescence | hydrothermal 3 h at 140 °C | | 0.376 nM | 4.5–6.5 nm | [166] |
| **Glucose N-CQD, B-CQD, and S-CQD** | $Fe^{3+}$,Ag+,$Ca^{2+}$ | colorimetric | hydrothermal process 200°C for 6h | | 0.187mM(Fe3+) 0.391mM(Ca2+) –0.442mM(Ag+) | 5-7nm | [38] |
| **Polyalthia longifolia p-CQDs** | $Cd^{2+}$ | Fluorescent | hydrothermal 150 ◦C for 6h | 22% | 2.4 nM | Red 3.33 nm | [39] |
| **excess sludge ESCQDs** | heavy metal control | fluorescent | hydrothermal process 200 ℃, time varied | 28.472 % | | | [167] |
| **corncob** | $Pb^{2+,}$ $Cu^{2+}$, $Fe^{3+}$, and $Cr^{3+}$ | fluorescent | Hydrothermal 70–80◦C for 12 h | | 0.8550 µM/mL Fe3+, 2.8562 µM/mL Cr3+ | White ~4 nm | [168] |
| **cane molasses** | Ag+, $Hg^{2+}$and $Cu^{2+}$ | fluorescent | Hydrothermal 160 ◦C for 24 h | | | 1.7 nm blue | [169] |
| **5-dimethyl amino methyl furfuryl alcohol and o-phenylene diamine** | $Hg^{2+}$ | fluorescent | Hydrothermal 160 °C for 4 hr | 12.0% | 5.2 nM | Yellow 2.6-3.4 nm | [170] |
| **L-tryptophan-mediated CQDs** | $Fe^{3+}$ and $Hg^{2+}$ | fluorescent | Hydrothermal | 7.6 % | $1.2\times10^{-5}$M and $1.9\times10^{-5}$ M | Blue 3.0-5.1 nm. | [171] |
| **Bombax ceiba stem** | $Fe^{3+}$/$Cd^{2+}$ | fluorescent | Hydrothermal | | 1.9 µM | Blue 6.5 nm | [3] |
| **Litsea glutinosa stem** | $Cu^{2+}$/$Hg^{2+}$ | fluorescent | Hydrothermal | | 0.1 µM and 0.2 µM | Green 7.5 nm | [12] |

absorption of light. This energy is then transferred to the quencher upon the collision between the excited fluorophore and quencher, leading to decreased fluorescence [158]. This process is concentration-dependent and can be reversed. For all the types of collisions, the number of such collisions grows with the increase in temperature.

In recent years, CQDs have been extensively explored for heavy metal ion detection in aqueous environments, driven by increasing concerns over water pollution and public health. Toxic metal ions such as $Hg^{2+}$, $Pb^{2+}$, $Cd^{2+}$, $Cu^{2+}$, $Fe^{3+}$, and $Cr^{6+}$ are persistent environmental contaminants that pose serious risks even at trace levels [159]. CQDs synthesised via sustainable and green routes have demonstrated exceptional sensitivity toward these ions, often achieving detection limits in the nano- to micromolar range [12],[148].

The strong affinity between metal ions and surface functional groups on CQDs enables efficient fluorescence modulation, primarily through quenching mechanisms. For instance, metal ions with high coordination tendencies can interact with carboxyl or amino groups on CQD surfaces, facilitating non-radiative recombination pathways and resulting in pronounced fluorescence suppression [3]. In some cases, fluorescence enhancement has also been observed due to surface passivation or aggregation-induced emission effects [160]. Importantly, the low cytotoxicity, excellent water solubility, and chemical stability of CQDs make them particularly suitable for environmental monitoring applications [161].

Despite the growing number of reports on CQD-based fluorescence sensors, systematic comparisons of their analytical performance, particularly for heavy metal detection, remain limited. Parameters such as limit of detection, linear response range, selectivity, reproducibility, and recovery efficiency vary significantly depending on synthesis methods, surface chemistry, and sensing mechanisms. A consolidated evaluation of these factors is necessary to identify performance trends and guide the rational design of next-generation CQD sensors.

To better illustrate the current state of research and identify emerging trends, Table 3 presents a representative selection of fluorescence-based carbon quantum dot sensors reported for heavy metal ion detection in water. The compiled studies reflect the diversity of sustainable carbon precursors and synthesis routes employed, as well as the resulting variations in sensing performance toward different metal ions. Collectively, these reports demonstrate that CQD surface chemistry and preparation strategy play a decisive role in determining sensitivity and selectivity, particularly for transition and post-transition metal ions. The comparison also reveals a general trend toward lower detection limits and improved performance when biomass-derived CQDs with abundant surface functional groups are employed, underscoring their suitability for environmentally relevant water monitoring applications.

### 7.1. Mercury ($Hg^{2+}$) Ions

$Hg^{2+}$ is one of the most harmful heavy metals due to its high neurotoxicity, bioaccumulation and because it binds firmly with thiol containing biomolecules, causing irreversible damage to both the nervous and the renal systems [172]. The most frequent technologies are chemical precipitation (insoluble $HgS/Hg(OH)_2$ formation), activated carbon adsorption, ion exchange, and membrane filtration. Although effective in high concentrations, they are poor in selectivity at trace levels, form secondary sludge, are expensive to operate and have complex regeneration. Moreover, the high affinity of $Hg^{2+}$ with natural organic matter tends to lower the removal efficiency.

Despite these dangers, mercury remains widely used in industrial activities such as colour-alkali production, battery manufacturing, and electronic industries, increasing the likelihood of its release into aquatic environments. Therefore, continuous and sensitive monitoring of water resources near industrial regions is essential to prevent mercury-related ecological and health impacts [173].

CQDs and especially sulfur or nitrogen doped CQDs are rich in the number of-SH, $-NH_2$ or -COOH groups that strongly coordinate with the soft Lewis acid $Hg^{2+}$. The two main routes are surface complexation, chelation, and, in many cases, after formation of ground-state complexes, the electron transfer via photoinduced electron transfer (PET) or via static quenching [174]. Excessive specificity of $Hg^{2+}$ and sulfur functionalities is improved in multi-ion systems. CQDs can be produced to recognise and capture ultra-low concentrations of a molecule at once, unlike precipitation, and do not form toxic by-products.

In one study, sulfhydryl-functionalized carbon quantum dots (HS-CQDs) were synthesised via a straightforward one-pot hydrothermal route and employed as a fluorescent “turn-off” probe for mercury ions ($Hg^{2+}$). The introduction of –SH groups on the CQD surface enhanced the binding affinity toward $Hg^{2+}$, facilitating the formation of non-fluorescent complexes and promoting electron transfer that leads to fluorescence quenching [175]. These HS-CQDs showed a good linear response to $Hg^{2+}$ concentrations between 0.45 and 2.1 µM and achieved a low detection limit of 12 nM, demonstrating the system’s high sensitivity. The practical applicability of this sensor was further validated through the successful detection of $Hg^{2+}$ in real environmental samples, showcasing its potential utility for monitoring mercury contamination in water matrices [175].

Xiang, Jun, et al. synthesised biomass-derived carbon dots from Chenpi (dried citrus peel) via a green hydrothermal approach, serving as label-free fluorescent probes for mercury detection. These biomass CQDs displayed strong fluorescence emission and excellent stability in aqueous environments, and their photoluminescence intensity decreased in the presence of $Hg^{2+}$ ions due to effective quenching interactions. The fluorescence response exhibited a clear linear relationship over the concentration range of 10–300 nM, with a remarkably low detection limit of approximately 7.0 nM, indicating highly sensitive detection capabilities [176].

### 7.2. Lead ($Pb^{2+}$) Ion

$Pb^{2+}$ exposure leads to developmental defects, neurological dysfunction, and cardiovascular toxicity, especially in children. It is very persistent and mobile in water systems and thus continuous monitoring is necessary. It primarily exists in three oxidation states: Pb(0), Pb(II), and Pb(IV). A major contributor to lead contamination in drinking water is the corrosion of pipes and plumbing fixtures containing lead, especially under acidic conditions [177]. The permissible concentration of lead in drinking water has been reported to be approximately 15 ppb [178]. Various inorganic nanomaterials, including ZnS, gold nanoparticles, CdS, polymer dots, and enzyme-based sensors, have been explored as fluorescent probes for detecting $Pb^{2+}$ ions. However, these approaches are often limited by high costs. Consequently, the development of cost-effective and environmentally friendly sensing materials remains an active research area [179].

Commonly used methods include precipitation, coagulation, flocculation, electrochemical treatment and adsorption on clays or biosorbents [180]. These techniques are usually however slow kinetics, low efficiency below ppm-ppb, and highly pH dependent. Sludge control and cation exchange are also significant disadvantages.

The presence of oxygen and nitrogen functional groups on the surface of CQD allows several coordination sites with $Pb^{2+}$. The usual result of binding is either PET or static quenching as a result of the donation of electrons to the empty orbitals of $Pb^{2+}$ by surface ligands [181]. Heteroatom doping enhances the density of charges and stability of the complex, which is reflected in the minimum detection and selectivity.

For instance, Kumar et al. synthesised CQDs using *Ocimum sanctum* and applied them to detect $Pb^{2+}$ in real water samples. They observed fluorescence quenching in the presence of $Pb^{2+}$ ions, achieving a detection limit of 0.59 nM and a quantum yield of 9.3%. This quenching was attributed to electron–hole recombination, resulting from the strong interaction between the empty d-orbitals of $Pb^{2+}$ ions and the amine groups on the CQD surface [182].

Nitrogen-doped CQDs (N-CQDs) prepared from *Lantana camara* berries have been investigated in detail to understand both dynamic and static fluorescence quenching mechanisms. Stern–Volmer analysis at multiple temperatures indicated a direct correlation between quenching constant and temperature. These N-CQDs effectively detect $Pb^{2+}$ in human urine, serum, and water samples, with a notable decrease in fluorescence intensity at 450 nm as $Pb^{2+}$ concentration increased, demonstrating high selectivity [183].

CQDs with an average size of 3.5 nm, synthesised from sugar, also show potential for $Pb^{2+}$ detection. Fluorescence quenching in these CQDs occurs through carboxylate-induced aggregation, which was confirmed using FTIR and XRD analyses. They have been successfully applied to detect $Pb^{2+}$ in real water samples [184]. Additionally, CQDs derived from bamboo leaves have been utilised for selective $Pb^{2+}$ detection in river water, offering practical applications in environmental monitoring and water safety management [185].

### 7.3. Copper ($Cu^{2+}$) Ion

Copper is a naturally occurring heavy metal that is widespread in the environment and plays a vital biological role. It acts as an essential mineral, facilitating various enzymatic functions in plants and animals [186]. However, excessive copper exposure can be toxic, highlighting the importance of monitoring its levels in both ecosystems and living organisms. This has led to numerous studies focused on developing effective methods for Cu detection, with CQDs emerging as a promising approach for this purpose [187].

Chauhan et al. reported a dual "turn-on/off" sensor for $Cu^{2+}$ and $Cd^{2+}$ detection in aqueous solutions, using CDs derived from coconut coir via thermal calcination. In their study, $Cu^{2+}$ ions caused quenching of the CD fluorescence, whereas $Cd^{2+}$ induced an enhancement of fluorescence intensity. These changes were attributed to interactions between the metal ions and oxygen-containing groups on the CD surface: $Cu^{2+}$ promoted non-radiative charge recombination leading to quenching, while $Cd^{2+}$ increased the intrinsic radiative decay rate, enhancing fluorescence. The detection limits for $Cu^{2+}$ and $Cd^{2+}$ were found to be 0.28 nM and 0.18 nM, respectively, demonstrating the sensor's applicability for monitoring these metals in wastewater [188].

A fluorescent paper-based CD sensor was also developed to detect $Cu^{2+}$ ions in water through the photoinduced electron transfer (PET) mechanism [189]. The CDs were synthesized hydrothermally using radish as a precursor, resulting in CDs rich in functional groups capable of chelating $Cu^{2+}$ and forming complexes that quenched fluorescence. The sensor exhibited a linear response for $Cu^{2+}$ concentrations between 10–60 μM, with a limit of detection of 6.8 μM, and was successfully applied to real water samples. Additionally, this sensor demonstrated potential for acetic acid vapour detection [189].

Blue-emitting CDs (BCDs) were fabricated using palm kernel shell and urea via microwave irradiation [190]. When tested in aqueous media, $Cu^{2+}$ ions induced significant fluorescence quenching, which was attributed to electrostatic interactions between the metal ions and CDs. The CDs could detect $Cu^{2+}$ over a 0–0.5 mM concentration range, with a detection limit of 0.05 mM. Beyond sensing, these BCDs were further employed for bacterial cell imaging and as fluorescent inks, highlighting their utility as reliable tools for monitoring Cu in environmental and biological systems [190].

### 7.4. Iron (Fe) Ion

Iron (Fe), despite being vital biologically, surplus $Fe^{3+}$ can prominently drive the generation of reactive oxygen species, resulting in oxidative stress, organ injury, and a decrease in water quality. In aquatic environments, iron is frequently detected in drinking water and municipal wastewater, particularly in regions influenced by iron- and steel-related industrial activities. The average daily iron intake for humans typically falls within the range of 10–50 mg [191]. According to the U.S. Environmental Protection Agency (EPA), a secondary maximum contaminant level of 0.3 ppm has been recommended for iron in drinking water, as elevated concentrations may lead to undesirable effects such as metallic taste, discolouration, and staining of plumbing fixtures. Although iron concentrations up to approximately 2 ppm are generally regarded as safe, prolonged exposure to higher levels can result in excessive iron accumulation in the body, potentially causing serious health disorders, including hemochromatosis, liver cirrhosis, and diabetes mellitus [192]. Treatment of iron is normally done through oxidation-precipitation or filtration. These are non-selective and simple but ineffective processes of differentiating between oxidation states. They are also highly pH-sensitive and cannot be used in complex matrices [193].

$Fe^{3+}$ is highly attracted to carboxyl groups and hydroxyl groups; thus, surface coordination with CQDs can take place quickly. Due to the potency of $Fe^{3+}$ as an electron acceptor, fluorescence response is often directed by dynamic quenching or PET, in the presence or absence of aggregation. The non-radiative relaxation in $Fe^{3+}$ is further enhanced by its paramagnetic feature, making it highly sensitive even in very low concentrations [194].

Song, Yuanyuan, et al. have synthesised wool keratin-derived nitrogen and sulfur co-doped CQDs via a simple hydrothermal method and exhibit excitation-dependent fluorescence behaviour. These nanoprobes demonstrate selective quenching of their fluorescence signal in the presence of $Fe^{3+}$, attributed to specific interactions between metal ions and functional groups (e.g., carboxyl and amino groups) on the CQD surface. The quenching response shows a clear, approximately linear correlation with $Fe^{3+}$ concentration, indicating the potential of such green CQDs for rapid and selective detection of ferric ions in environmental water samples. The study also emphasises that the presence of other metal ions does not significantly interfere with the sensing performance, underscoring the selectivity of the CQD probe for iron ions under practical conditions [195].

For instance, Zhao, Pei, et al. used water hyacinth, a highly abundant aquatic plant, as a sustainable carbon source for the hydrothermal preparation of fluorescent carbon dots. These water hyacinth-derived CQDs displayed uniform particle size, strong blue photoluminescence, and excellent dispersibility in water [196]. When introduced to solutions containing $Fe^{3+}$ ions, the fluorescence intensity of the CQDs decreased progressively with increasing ion concentration, enabling selective and sensitive detection. Notably, the detection limit achieved for $Fe^{3+}$ with these biomass CQDs was

as low as approximately 0.084 µM, with a broad linear response range up to several hundred micromolars, values that are well below typical regulatory thresholds for safe drinking water [196].

### 7.5. Chromium ($Cr^{2+}$) Ion

In aquatic systems, chromium is mainly found as trivalent [Cr(III)] and hexavalent [Cr(VI)] forms, which differ significantly in their biological and environmental effects [197]. While Cr(III) is an essential micronutrient important for animal growth and metabolism, Cr(VI) is highly toxic, exhibiting carcinogenic, mutagenic, and teratogenic properties [198]. Its high environmental mobility further increases the risk of widespread contamination, making its removal from wastewater critical for environmental and public health [199].

Cost-effective carbon quantum dots (CQDs) have been synthesised from lemon peel waste, showing strong photoluminescence, high aqueous stability, and a quantum yield of ~14% [200]. These CQDs functioned as an eco-friendly fluorescent probe for Cr(VI) detection with a detection limit of 73 nM and high selectivity, offering a rapid and sensitive method for water monitoring [200]. Similarly, nitrogen-doped CQDs derived from sugarcane bagasse have been reported for Cr(VI) adsorption [201]. Kinetic studies indicated that adsorption follows both pseudo-first and pseudo-second-order models, with the latter providing a better fit, suggesting chemisorption as the dominant mechanism. Boyd model analysis confirmed that external diffusion governs the rate of Cr(VI) removal [201].

## 8. Challenges and Future Perspective

Despite the rapid progress in the development of biomass-derived fluorescent carbon quantum dots for heavy metal sensing, several challenges must be addressed before their full-scale practical implementation. One of the primary limitations is the difficulty in translating laboratory-scale synthesis into large-scale, commercially viable production. Although biomass precursors offer sustainability and low cost, achieving consistent quality, reproducibility, and batch-to-batch uniformity remains a significant hurdle for real-world deployment.

Another challenge lies in the relatively lower quantum yield of biomass-derived CQDs compared to chemically synthesised counterparts. While green synthesis routes reduce environmental impact, further optimization of reaction conditions, precursor selection, and surface passivation strategies is required to enhance fluorescence efficiency without compromising sustainability. In addition, the majority of existing studies focus on a limited number of metal ions, particularly $Fe^{3+}$, $Hg^{2+}$, and $Cu^{2+}$, leaving other environmentally hazardous metals insufficiently explored. Expanding CQD design toward target-specific sensing of a broader range of toxic ions remains an important research direction.

Selectivity is another critical concern, especially in complex water matrices containing multiple competing ions. A deeper understanding of metal–CQD interaction mechanisms, including fluorescence quenching pathways and surface binding phenomena, is essential for designing highly selective sensors. Furthermore, challenges related to purification, structural characterisation, and long-term stability must be resolved to ensure reliable performance in real environmental samples. The future perspectives of carbon quantum dots for sustainable synthesis and enhanced heavy metal detection are summarised in Figure 11.

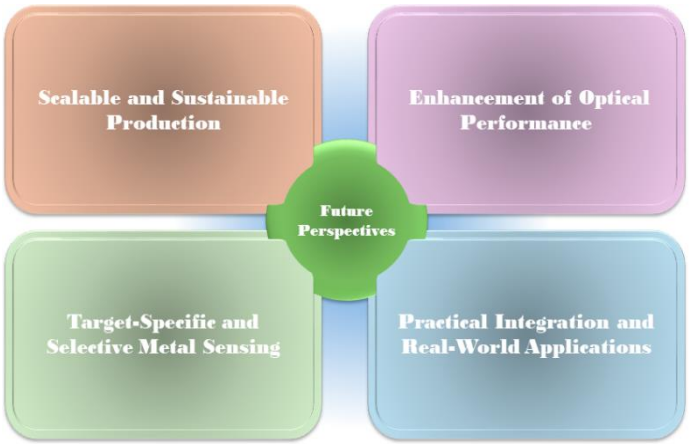


**Figure 11**: *Schematic representation illustrating the future perspectives of carbon quantum dots for sustainable synthesis, enhanced sensing performance, and practical heavy metal detection in water*

Future research should focus on rational surface engineering, heteroatom doping, and controlled synthesis using tailored biomass precursors to improve optical performance and metal specificity. Integrating CQDs into solid-state platforms, portable devices, and real-time monitoring systems will further enhance their applicability. Addressing these challenges will accelerate the transition of sustainable CQDs from experimental materials to practical tools for environmental monitoring.

## 9. Conclusion

This review highlights the significant progress toward the sustainable production of fluorescent carbon quantum dots and their growing role in heavy metal detection in water systems. Biomass-derived CQDs have emerged as an environmentally benign alternative to conventional semiconductor quantum dots, offering advantages such as low toxicity, biocompatibility, water solubility, and cost-effective synthesis from renewable resources. The bottom-up green synthesis approach, in particular, enables fine control over CQD surface chemistry and optical properties, which are critical for sensing applications.

The presence of diverse surface functional groups and the possibility of heteroatom doping allow CQDs to interact selectively with various heavy metal ions, making them highly sensitive fluorescent probes. Their low detection limits, photostability, and adaptability to different sensing environments underscore their potential for environmental applications. However, challenges related to large-scale production, fluorescence efficiency, selectivity in complex matrices, and mechanistic understanding still require focused investigation.

Overall, sustainable CQDs represent a promising platform for next-generation heavy metal sensors. Continued research into green synthesis strategies, surface functionalization, and sensing mechanisms will not only improve detection performance but also contribute to the development of eco-friendly technologies for water quality monitoring and environmental protection.

## Declaration

**AI Disclosure:** Artificial Intelligence (AI)-based tools were used in this study only as supportive instruments to improve the clarity and linguistic quality of the manuscript. AI was applied solely for grammatical correction, sentence refinement, and enhancement of readability. No AI tools were employed for content generation, experimental work, data analysis, interpretation of results, or formulation of scientific conclusions. All research findings,

analyses, and critical evaluations were conducted independently by the authors, who take full responsibility for the originality, accuracy, and ethical integrity of the manuscript.

**Author Contribution Statement:** M. A. A. contributed to conceptualization, data curation, formal analysis, and preparation of the original draft. J. A. was responsible for conceptualization, methodology development, visualization, data interpretation, and preparation of the original draft. A. R. provided visualization and technical support. R. contributed to visualization and technical assistance. All authors reviewed and approved the final manuscript.

**Competing Interests:** The authors declare that they have no known competing financial interests or personal relationships that could have appeared to influence the work reported in this paper.

**Consent to Publish:** The authors are agreed to publish version of the manuscript in this journal.

**Ethical Issues:** There are no ethical issues. All data in this paper is publicly available.

**Funding Statement:** This research did not receive any specific grant from funding agencies in the public, commercial, or not-for-profit sectors.

## References

1. Jayaprakash, N., et al., Carbon nanomaterials: revolutionizing biomedical applications with promising potential. 2024.
2. Wang, X., et al., A mini review on carbon quantum dots: preparation, properties, and electrocatalytic application. 2019. 7: p. 671.
3. Akhtar, M.A., et al., Eco-friendly synthesis of N-doped carbon quantum dots from Bombax ceiba stem: A photophysical study with exploratory sensing of Fe3+/Cd2+ and dye degradation. 2025. 78: p. 108704.
4. Cayuela, A., et al., Semiconductor and carbon-based fluorescent nanodots: the need for consistency. 2016. 52(7): p. 1311-1326.
5. Liu, M.L., et al., Carbon dots: synthesis, formation mechanism, fluorescence origin and sensing applications. 2019. 21(3): p. 449-471.
6. Hagiwara, K., S. Horikoshi, and N.J.C.A.E.J. Serpone, Photoluminescent carbon quantum dots: synthetic approaches and photophysical properties. 2021. 27(37): p. 9466-9481.
7. Shabbir, H., E. Csapó, and M.J.I. Wojnicki, Carbon quantum dots: the role of surface functional groups and proposed mechanisms for metal ion sensing. 2023. 11(6): p. 262.
8. Gulati, S., et al., Eco-friendly and sustainable pathways to photoluminescent carbon quantum dots (CQDs). 2023. 13(3): p. 554.
9. Dhariwal, J., G.K. Rao, and D.J.R.S. Vaya, Recent advancements towards the green synthesis of carbon quantum dots as an innovative and eco-friendly solution for metal ion sensing and monitoring. 2024. 2(1): p. 11-36.
10. Nguyen, K.G., et al., Investigating the effect of N-doping on carbon quantum dots structure, optical properties and metal ion screening. 2022. 12(1): p. 13806.
11. Xu, H., et al., Research on green synthesis and performance analysis of biomass-derived carbon quantum dots. 2025. 227: p. 120775.
12. Anum, J., et al., Green-synthesized amino-rich carbon quantum dots: A dual-function platform for fluorescent detection of heavy metals and degradation of malachite green dye. 2025. 77: p. 108472.
13. Zhu, L., et al., State-of-the-art on the preparation, modification, and application of biomass-derived carbon quantum dots. 2020. 59(51): p. 22017-22039.
14. Wu, J., et al., Synthesis and applications of carbon quantum dots derived from biomass waste: a review. 2023. 21(6): p. 3393-3424.
15. Šafranko, S., et al., An overview of the recent developments in carbon quantum dots—promising nanomaterials for metal ion detection and (bio) molecule sensing. 2021. 9(6): p. 138.
16. Singh, P., et al., Assessment of biomass-derived carbon dots as highly sensitive and selective templates for the sensing of hazardous ions. 2023. 15(40): p. 16241-16267.
17. Lim, S.Y., W. Shen, and Z.J.C.S.R. Gao, Carbon quantum dots and their applications. 2015. 44(1): p. 362-381.
18. Xu, Q., et al., Function-driven engineering of 1D carbon nanotubes and 0D carbon dots: mechanism, properties and applications. 2019. 11(4): p. 1475-1504.
19. Xu, X., et al., Electrophoretic analysis and purification of fluorescent single-walled carbon nanotube fragments. 2004. 126(40): p. 12736-12737.
20. Hu, S., et al., Laser synthesis and size tailor of carbon quantum dots. 2011. 13: p. 7247-7252.
21. Pillar-Little, T.J., et al., Superior photodynamic effect of carbon quantum dots through both type I and type II pathways: Detailed comparison study of top-down-synthesized and bottom-up-synthesized carbon quantum dots. 2018. 140: p. 616-623.
22. Yang, S., et al., Fabrication of carbon-based quantum dots via a “bottom-up” approach: Topology, chirality, and free radical processes in “Building Blocks”. 2023. 19(31): p. 2205957.
23. Kaur, I., et al., Chemical-and green-precursor-derived carbon dots for photocatalytic degradation of dyes. 2024. 27(2).
24. Nammahachak, N., et al., Hydrothermal synthesis of carbon quantum dots with size tunability via heterogeneous nucleation. 2022. 12(49): p. 31729-31733.
25. Lima-Tenorio, M.K., et al., Magnetic nanoparticles: In vivo cancer diagnosis and therapy. 2015. 493(1-2): p. 313-327.
26. Msto, R.K., et al., Fluorescence turns on-off-on sensing of ferric ion and L-ascorbic acid by carbon quantum dots. 2023. 2023(1): p. 5555608.
27. Arumugam, N. and J.J.M.L. Kim, Synthesis of carbon quantum dots from Broccoli and their ability to detect silver ions. 2018. 219: p. 37-40.
28. Atchudan, R., et al., Hydrophilic nitrogen-doped carbon dots from biowaste using dwarf banana peel for environmental and biological applications. 2020. 275: p. 117821.
29. Thakur, S., et al., Valorization of food industrial waste: Green synthesis of carbon quantum dots and novel applications. 2023: p. 140656.
30. Al-Douri, Y., N. Badi, and C.H.J.L. Voon, Synthesis of carbon-based quantum dots from starch extracts: Optical investigations. 2018. 33(2): p. 260-266.
31. Sadegh Hassani, S., et al., Carbon-based Quantum Dots from Food Waste: Synthesis to Application in Food Safety. 2023.
32. Park, S.J., et al., Color tunable carbon quantum dots from wasted paper by different solvents for anti-counterfeiting and fluorescent flexible film. 2020. 383: p. 123200.
33. Bhunia, S.K., et al., Carbon nanoparticle-based fluorescent bioimaging probes. 2013. 3(1): p. 1473.
34. Lu, Z., et al., Potential application of nitrogen-doped carbon quantum dots synthesized by a solvothermal method for detecting silver ions in food packaging. 2019. 16(14): p. 2518.
35. Singh, H., et al., One-pot hydrothermal synthesis and characterization of carbon quantum dots (CQDs). 2020. 28: p. 1891-1894.
36. Nan, Z., et al., Carbon quantum dots (CQDs) modified ZnO/CdS nanoparticles based fluorescence sensor for highly selective and sensitive detection of Fe (III). 2020. 228: p. 117717.
37. Khan, Z.M., et al., Hydrothermal treatment of red lentils for the synthesis of fluorescent carbon quantum dots and its application for sensing Fe3+. 2019. 91: p. 386-395.
38. Aygun, A., et al., Hydrothermal synthesis of B, S, and N-doped carbon quantum dots for colorimetric sensing of heavy metal ions. 2024. 14(16): p. 10814-10825.
39. Kolaprath, M.K.A., et al., A facile, green synthesis of carbon quantum dots from Polyalthia longifolia and its application for the selective detection of cadmium. 2023. 210: p. 111048.
40. Singh, R., et al., Progress in microwave-assisted synthesis of quantum dots (graphene/carbon/semiconducting) for bioapplications: a review. 2019. 12: p. 282-314.
41. Nadagouda, M.N., T.F. Speth, and R.S.J.A.o.C.R. Varma, Microwave-assisted green synthesis of silver nanostructures. 2011. 44(7): p. 469-478.
42. Bhattacharyya, S., et al., Effect of nitrogen atom positioning on the trade-off between emissive and photocatalytic properties of carbon dots. 2017. 8(1): p. 1401.

43. Nazar, M., et al., Microwave Synthesis of Carbon Quantum Dots from Arabica Coffee Ground for Fluorescence Detection of Fe3+, Pb2+, and Cr3+. 2024. 9(18): p. 20571-20581.
44. Architha, N., et al., Microwave-assisted green synthesis of fluorescent carbon quantum dots from Mexican Mint extract for Fe3+ detection and bio-imaging applications. 2021. 199: p. 111263.
45. Chugh, R. and G. Kaur, Citrus sinensis agro-waste peels mediated CQDs-Ag nanocomposite potentiates numerous applications. 2023.
46. Zaman, A.S.K., et al., Properties and molecular structure of carbon quantum dots derived from empty fruit bunch biochar using a facile microwave-assisted method for the detection of Cu2+ ions. 2021. 112: p. 110801.
47. Monte-Filho, S.S., et al., Synthesis of highly fluorescent carbon dots from lemon and onion juices for determination of riboflavin in multivitamin/mineral supplements. 2019. 9(3): p. 209-216.
48. Suppan, T., et al., Fluorescent 'turn-on'porphyrin CQD nanoprobes for selective sensing of heavy metal ions. 2024: p. 111265.
49. Kaur, R., et al., Waste biomass-derived CQDs and Ag-CQDs as a sensing platform for Hg2+ ions. 2022. 29: p. 100813.
50. Kumari, A., et al., Synthesis of green fluorescent carbon quantum dots using waste polyolefins residue for Cu2+ ion sensing and live cell imaging. 2018. 254: p. 197-205.
51. Zhou, J., et al., Facile synthesis of fluorescent carbon dots using watermelon peel as a carbon source. 2012. 66(1): p. 222-224.
52. Abid, N., et al., Synthesis of nanomaterials using various top-down and bottom-up approaches, influencing factors, advantages, and disadvantages: A review. 2022. 300: p. 102597.
53. Sajini, T. and J.J.R.S. Joseph, Microwave-assisted synthesis of nanomaterials: a green chemistry perspective and sustainability assessment. 2025. 3(11): p. 4911-4935.
54. Kim, H.H., et al., Bottom-up synthesis of carbon quantum dots with high performance photo-and electroluminescence. 2018. 35(7): p. 1800080.
55. Ray, S., et al., Fluorescent carbon nanoparticles: synthesis, characterization, and bioimaging application. 2009. 113(43): p. 18546-18551.
56. Shaik, S.A., et al., Syntheses of N-doped carbon quantum dots (NCQDs) from bioderived precursors: a timely update. 2020. 9(1): p. 3-49.
57. El-Shabasy, R.M., et al., Recent developments in carbon quantum dots: properties, fabrication techniques, and bio-applications. 2021. 9(2): p. 388.
58. Wang, C., et al., Carbon quantum dots prepared by pyrolysis: investigation of the luminescence mechanism and application as fluorescent probes. 2022. 204: p. 110431.
59. Namdari, P., et al., Synthesis, properties and biomedical applications of carbon-based quantum dots: An updated review. 2017. 87: p. 209-222.
60. Dhandapani, E., N. Duraisamy, and P.J.M.T.P. Periasamy, Highly green fluorescent carbon quantum dots synthesis via hydrothermal method from fish scale. 2020. 26: p. A1-A5.
61. Ou, S.-F., et al., N-doped carbon quantum dots as fluorescent bioimaging agents. 2021. 11(7): p. 789.
62. Saikia, T., J. Al-Jaberi, and A.J.A.o. Sultan, Synthesis and testing of monoethylene glycol carbon quantum dots for inhibition of hydrates in CO2 sequestration. 2021. 6(23): p. 15136-15146.
63. Tang, L., et al., Deep ultraviolet photoluminescence of water-soluble self-passivated graphene quantum dots. 2012. 6(6): p. 5102-5110.
64. Hola, K., et al., Photoluminescence effects of graphitic core size and surface functional groups in carbon dots: COO− induced red-shift emission. 2014. 70: p. 279-286.
65. Dager, A., et al., Synthesis and characterization of mono-disperse carbon quantum dots from fennel seeds: photoluminescence analysis using machine learning. 2019. 9(1): p. 14004.
66. Martindale, B.C., et al., Enhancing light absorption and charge transfer efficiency in carbon dots through graphitization and core nitrogen doping. 2017. 129(23): p. 6559-6563.
67. Zhang, W., et al., Large-area color controllable remote carbon white-light light-emitting diodes. 2015. 85: p. 344-350.
68. Yu, T., et al., A rapid microwave synthesis of green-emissive carbon dots with solid-state fluorescence and pH-sensitive properties. 2018. 5(7): p. 180245.
69. Kaur, G.A., et al., Structural and optical amendment of PVDF into CQDs through high temperature calcination process. 2021. 304: p. 130616.
70. Hu, S.-L., et al., One-step synthesis of fluorescent carbon nanoparticles by laser irradiation. 2009. 19(4): p. 484-488.
71. Hou, H., et al., Carbon quantum dots and their derivative 3D porous carbon frameworks for sodium-ion batteries with ultralong cycle life. 2015. 27(47): p. 7861-7866.
72. Arumugham, T., et al., A sustainable synthesis of green carbon quantum dot (CQD) from Catharanthus roseus (white flowering plant) leaves and investigation of its dual fluorescence responsive behavior in multi-ion detection and biological applications. 2020. 23: p. e00138.
73. Qiang, S., et al., New insights into the cellular toxicity of carbon quantum dots to Escherichia coli. 2022. 11(12): p. 2475.
74. Kolanowska, A., et al., Carbon quantum dots from amino acids revisited: Survey of renewable precursors toward high quantum-yield blue and green fluorescence. 2022. 7(45): p. 41165-41176.
75. Chandra, S., et al., Tuning of photoluminescence on different surface functionalized carbon quantum dots. 2012. 2(9): p. 3602-3606.
76. Luo, P.G., et al., Carbon "quantum" dots for optical bioimaging. 2013. 1(16): p. 2116-2127.
77. Arul, V., et al., Optical and Biomedical Features of Green Carbon Quantum Dots, in Green Carbon Quantum Dots: Environmental Applications. 2024, Springer. p. 85-116.
78. Tejwan, N., et al., Multifaceted applications of green carbon dots synthesized from renewable sources. 2020. 275: p. 102046.
79. Sun, Y.-P., et al., Quantum-sized carbon dots for bright and colorful photoluminescence. 2006. 128(24): p. 7756-7757.
80. Atchudan, R., et al., Green synthesized multiple fluorescent nitrogen-doped carbon quantum dots as an efficient label-free optical nanoprobe for in vivo live-cell imaging. 2019. 372: p. 99-107.
81. Ding, H., et al., Surface states of carbon dots and their influences on luminescence. 2020. 127(23).
82. Pan, J., et al., A novel and sensitive fluorescence sensor for glutathione detection by controlling the surface passivation degree of carbon quantum dots. 2017. 166: p. 1-7.
83. Omer, K.M.J.A. and b. chemistry, Highly passivated phosphorous and nitrogen co-doped carbon quantum dots and fluorometric assay for detection of copper ions. 2018. 410: p. 6331-6336.
84. Wang, F., et al., One-step synthesis of highly luminescent carbon dots in noncoordinating solvents. 2010. 22(16): p. 4528-4530.
85. Dong, Y., et al., Carbon-based dots co-doped with nitrogen and sulfur for high quantum yield and excitation-independent emission. 2013. 52(30).
86. Anilkumar, P., et al., Toward quantitatively fluorescent carbon-based "quantum" dots. 2011. 3(5): p. 2023-2027.
87. Wang, H., et al., High fluorescence S, N co-doped carbon dots as an ultra-sensitive fluorescent probe for the determination of uric acid. 2016. 155: p. 62-69.
88. Bourlinos, A.B., et al., Green and simple route toward boron doped carbon dots with significantly enhanced non-linear optical properties. 2015. 83: p. 173-179.
89. Zhou, J., et al., Facile synthesis of P-doped carbon quantum dots with highly efficient photoluminescence. 2014. 4(11): p. 5465-5468.
90. Qu, S., et al., Toward efficient orange emissive carbon nanodots through conjugated sp (2)-domain controlling and surface charges engineering. 2016.
91. Farshbaf, M., et al., Carbon quantum dots: recent progresses on synthesis, surface modification and applications. 2018. 46(7): p. 1331-1348.
92. Molaei, M.J.J.S.E., The optical properties and solar energy conversion applications of carbon quantum dots: A review. 2020. 196: p. 549-566.
93. Zhang, Z., et al., Progress of carbon quantum dots in photocatalysis applications. 2016. 33(8): p. 457-472.
94. Baker, S.N. and G.A.J.A.C.I.E. Baker, Luminescent carbon nanodots: emergent nanolights. 2010. 49(38): p. 6726-6744.
95. Gokus, T., et al., Making graphene luminescent by oxygen plasma treatment. 2009. 3(12): p. 3963-3968.
96. Cao, L., et al., Photoluminescence properties of graphene versus other carbon nanomaterials. 2013. 46(1): p. 171-180.
97. Yuan, F., et al., Bright multicolor bandgap fluorescent carbon quantum dots for electroluminescent light-emitting diodes. 2017. 29(3): p. 1604436.
98. Srivastava, I., et al., Rational design of surface-state controlled multicolor cross-linked carbon dots with distinct photoluminescence and cellular uptake properties. 2021. 13(50): p. 59747-59760.

99. Chan, K.K., S.H.K. Yap, and K.-T.J.N.-m.l. Yong, Biogreen synthesis of carbon dots for biotechnology and nanomedicine applications. 2018. 10: p. 1-46.
100. Park, Y., et al., Improving the functionality of carbon nanodots: doping and surface functionalization. 2016. 4(30): p. 11582-11603.
101. Zhang, F., et al., Photoluminescent carbon quantum dots as a directly film-forming phosphor towards white LEDs. 2016. 8(16): p. 8618-8632.
102. Fang, L.-y. and J.-t.J.N.C.M. Zheng, Carbon quantum dots: Synthesis and correlation of luminescence behavior with microstructure. 2021. 36(3): p. 625-631.
103. Cao, L., et al., Carbon dots for multiphoton bioimaging. 2007. 129(37): p. 11318-11319.
104. Kong, B., et al., Carbon dot-based inorganic–organic nanosystem for two-photon imaging and biosensing of pH variation in living cells and tissues. 2012. 24(43): p. 5844.
105. Li, M., et al., Controlling the up-conversion photoluminescence property of carbon quantum dots (CQDs) by modifying its surface functional groups for enhanced photocatalytic performance of CQDs/BiVO4 under a broad-spectrum irradiation. 2021. 47(8): p. 3469-3485.
106. Yuan, T., et al., Carbon quantum dots: an emerging material for optoelectronic applications. 2019. 7(23): p. 6820-6835.
107. He, P., et al., Growing carbon quantum dots for optoelectronic devices. 2018. 34(11): p. 1250-1263.
108. Dave, K. and V.G.J.N.E. Gomes, Carbon quantum dot-based composites for energy storage and electrocatalysis: Mechanism, applications and future prospects. 2019. 66: p. 104093.
109. Samantara, A.K., et al., Sandwiched graphene with nitrogen, sulphur co-doped CQDs: an efficient metal-free material for energy storage and conversion applications. 2015. 3(33): p. 16961-16970.
110. Chen, J. and K.J.M.C.F. Rong, Nanophotonic devices and circuits based on colloidal quantum dots. 2021. 5(12): p. 4502-4537.
111. Kim, J., et al., Recent progress of quantum dot-based photonic devices and systems: a comprehensive review of materials, devices, and applications. 2021. 2(3): p. 2000024.
112. Arul, V., et al., Carbon quantum dots for smart electronic devices, in Green Carbon Quantum Dots: Environmental Applications. 2024, Springer. p. 367-386.
113. Li, H., et al., Carbon quantum dots/TiO x electron transport layer boosts efficiency of planar heterojunction perovskite solar cells to 19%. 2017. 17(4): p. 2328-2335.
114. Naushad, M., et al., Nitrogen-doped carbon quantum dots (N-CQDs)/Co3O4 nanocomposite for high performance supercapacitor. 2021. 33(1): p. 101252.
115. Guo, R., et al., Functionalized carbon dots for advanced batteries. 2021. 37: p. 8-39.
116. Zhu, Y., et al., A carbon quantum dot decorated RuO 2 network: outstanding supercapacitances under ultrafast charge and discharge. 2013. 6(12): p. 3665-3675.
117. Rasal, A.S., et al., Carbon quantum dots for energy applications: a review. 2021. 4(7): p. 6515-6541.
118. Rooj, B. and U.J.V.J.o.C. Mandal, A review on characterization of carbon quantum dots. 2023. 61(6): p. 693-718.
119. Hu, Q., et al., Characterization and analytical separation of fluorescent carbon nanodots. 2017. 2017(1): p. 1804178.
120. Song, X., et al., Pressure-assisted preparation of graphene oxide quantum dot-incorporated reverse osmosis membranes: antifouling and chlorine resistance potentials. 2016. 4(43): p. 16896-16905.
121. Saikia, M., et al., Feasibility study of preparation of carbon quantum dots from Pennsylvania anthracite and Kentucky bituminous coals. 2019. 243: p. 433-440.
122. Lim, H., et al., Facile synthesis and characterization of carbon quantum dots and photovoltaic applications. 2018. 660: p. 672-677.
123. Cheng, C., et al., Carbon quantum dots from carbonized walnut shells: Structural evolution, fluorescence characteristics, and intracellular bioimaging. 2017. 79: p. 473-480.
124. Ali, M., et al., Gradient heating-induced bi-phase synthesis of carbon quantum dots (CQDs) on graphene-coated carbon cloth for efficient photoelectrocatalysis. 2022. 196: p. 649-662.
125. Baslak, C., et al., Green synthesis capacitor of carbon quantum dots from Stachys euadenia. 2024. 43(3): p. e14340.
126. Jawad, M.M. and L.A.J.J.o.O. Abdullah, Novel characteristics of CQDs synthesized by electrochemical method. 2024: p. 1-9.
127. Butt, H.-J., B. Cappella, and M.J.S.s.r. Kappl, Force measurements with the atomic force microscope: Technique, interpretation and applications. 2005. 59(1-6): p. 1-152.
128. Moraille, P., et al., Experimental methods in chemical engineering: Atomic force microscopy− AFM. 2022. 100(10): p. 2778-2806.
129. Thambiraj, S. and R.J.A.S.S. Shankaran, Green synthesis of highly fluorescent carbon quantum dots from sugarcane bagasse pulp. 2016. 390: p. 435-443.
130. Wang, Y. and A.J.J.o.M.C.C. Hu, Carbon quantum dots: synthesis, properties and applications. 2014. 2(34): p. 6921-6939.
131. Yang, Q., et al., Nitrogen-doped carbon quantum dots from biomass via simple one-pot method and exploration of their application. 2018. 434: p. 1079-1085.
132. Tian, J., et al., Carbon quantum dots/hydrogenated TiO2 nanobelt heterostructures and their broad spectrum photocatalytic properties under UV, visible, and near-infrared irradiation. 2015. 11: p. 419-427.
133. Ateia, E.E., O. Rabie, and A.T.J.T.E.P.J.P. Mohamed, Assessment of the correlation between optical properties and CQD preparation approaches. 2024. 139(1): p. 1-12.
134. Bano, D., et al., Green synthesis of fluorescent carbon quantum dots for the detection of mercury (II) and glutathione. 2018. 42(8): p. 5814-5821.
135. Naik, V., et al., Nitrogen-doped carbon dots via hydrothermal synthesis: naked eye fluorescent sensor for dopamine and used for multicolor cell imaging. 2019. 2(5): p. 2069-2077.
136. ReddyPrasad, P. and E.B.J.J.o.M.S. Naidoo, Ultrasonic synthesis of high fluorescent C-dots and modified with CuWO4 nanocomposite for effective photocatalytic activity. 2015. 1098: p. 146-152.
137. Sha, Y., et al., Hydrothermal synthesis of nitrogen-containing carbon nanodots as the high-efficient sensor for copper (II) ions. 2013. 48(4): p. 1728-1731.
138. Peng, J., et al., Graphene quantum dots derived from carbon fibers. 2012. 12(2): p. 844-849.
139. Sooryakanth, B., et al., Sustainable Conversion of Chitosan Waste into Nitrogen-Doped Graphene Quantum Dots: Green Synthesis Pathways and Biomedical Potential. 2025. 2(3): p. 173-199.
140. Liu, Z., et al., Photoluminescence of carbon quantum dots: coarsely adjusted by quantum confinement effects and finely by surface trap states. 2018. 61(4): p. 490-496.
141. Yu, J., et al., Unveiling the quenching mechanism of metal ions using solvent-driven N, S-doped carbon quantum dots. 2025. 162: p. 116948.
142. Lai, S., et al., Fluorescence sensing mechanisms of versatile graphene quantum dots toward commonly encountered heavy metal ions. 2023. 8(10): p. 3812-3823.
143. Wang, F., et al., Application of carbon quantum dots as fluorescent probes in the detection of antibiotics and heavy metals. 2025. 463: p. 141122.
144. Gao, Y., et al., Carbon quantum dots in spectrofluorimetric analysis: A comprehensive review of synthesis, mechanisms and multifunctional applications. 2025: p. 128066.
145. Preeyanka, N. and M.J.L. Sarkar, Probing how various metal ions interact with the surface of QDs: implication of the interaction event on the photophysics of QDs. 2021. 37(23): p. 6995-7007.
146. Lee-Montiel, F.T. and P.J.J.o.M.C.B. Imoukhuede, Engineering quantum dot calibration standards for quantitative fluorescent profiling. 2013. 1(46): p. 6434-6441.
147. Sun, H. and P.J.J.o.M.S. Wu, Tuning the functional groups of carbon quantum dots in thin film nanocomposite membranes for nanofiltration. 2018. 564: p. 394-403.
148. Molaei, M.J.J.A.M., Principles, mechanisms, and application of carbon quantum dots in sensors: a review. 2020. 12(10): p. 1266-1287.
149. Liang, Z., et al., Probing energy and electron transfer mechanisms in fluorescence quenching of biomass carbon quantum dots. 2016. 8(27): p. 17478-17488.
150. Zu, F., et al., The quenching of the fluorescence of carbon dots: a review on mechanisms and applications. 2017. 184(7): p. 1899-1914.
151. Mo, X., Fluorescent Carbon Quantum Dots Probe for Detection of Deoxygenated Hemoglobin. 2024, National University of Singapore (Singapore).
152. Kou, X., et al., A review: recent advances in preparations and applications of heteroatom-doped carbon quantum dots. 2020. 49(21): p. 6915-6938.

153. Lakowicz, J.R. and J.R.J.P.o.f.s. Lakowicz, Quenching of fluorescence. 1983: p. 257-301.
154. Genovese, D., et al., Static quenching upon adduct formation: a treatment without shortcuts and approximations. 2021. 50(15): p. 8414-8427.
155. Ding, G., et al., Recent advances in carbon quantum dots for antibiotics detection. 2024(0).
156. Sudewi, S., et al., Understanding Antibiotic Detection with Fluorescence Quantum Dots: A Review. 2024: p. 1-25.
157. Sedlář, O., et al., Long-Term Application of Organic Fertilizers in Relation to Soil Organic Matter Quality. 2023. 13(1): p. 175.
158. Liu, Y., et al., N-Doping CQDs as an efficient fluorescence probe based on dynamic quenching for determination of copper ions and alcohol sensing in baijiu. 2025. 35(5): p. 3239-3251.
159. Järup, L.J.B.m.b., Hazards of heavy metal contamination. 2003. 68(1): p. 167-182.
160. Sekar, A., R. Yadav, and N.J.N.J.o.C. Basavaraj, Fluorescence quenching mechanism and the application of green carbon nanodots in the detection of heavy metal ions: a review. 2021. 45(5): p. 2326-2360.
161. Yao, K., et al., Effects of carbon quantum dots on aquatic environments: comparison of toxicity to organisms at different trophic levels. 2018. 52(24): p. 14445-14451.
162. Singh, J., et al., Highly fluorescent carbon dots derived from Mangifera indica leaves for selective detection of metal ions. 2020. 720: p. 137604.
163. Chaudhary, N., et al., One-step green approach to synthesize highly fluorescent carbon quantum dots from banana juice for selective detection of copper ions. 2020. 8(3): p. 103720.
164. Xiang-Yi, D., et al., Synthesis of functionalized carbon quantum dots as fluorescent probes for detection of Cu2+. 2020. 48(10): p. e20126-e20133.
165. Song, Z., et al., Luminescent carbon quantum dots/nanofibrillated cellulose composite aerogel for monitoring adsorption of heavy metal ions in water. 2020. 100: p. 109642.
166. Panda, S., et al., CQD@ γ-Fe2O3 multifunctional nanoprobe for selective fluorescence sensing, detoxification and removal of Hg (II). 2020. 589: p. 124445.
167. Han, Y., et al., Green conversion of excess sludge to N-Ca self-doping sustainable carbon quantum dots with remarkable fluorescence enhancement and residual heavy metal reduction. 2022. 10(6): p. 108934.
168. Jagannathan, M., et al., Green synthesis of white light emitting carbon quantum dots: Fabrication of white fluorescent film and optical sensor applications. 2021. 416: p. 125091.
169. Fan, X., et al., Chiral CQD-based PL and CD sensors for high sensitive and selective detection of heavy metal ions. 2023. 137: p. 113620.
170. Jaison, A.M.C., et al., One pot hydrothermal synthesis and application of bright-yellow-emissive carbon quantum dots in Hg2+ detection. 2023. 33(6): p. 2281-2294.
171. Zalmi, G.A., et al., Hydrothermal Synthesis of Tartaric Acid Functionalized Amino Acid CQD for Sensing of Hg2+ and Fe3+ Ions in Aqueous Medium. 2024. 9(18): p. e202304825.
172. Cohen, J.T., D.C. Bellinger, and B.A.J.A.j.o.p.m. Shaywitz, A quantitative analysis of prenatal methyl mercury exposure and cognitive development. 2005. 29(4): p. 353-353. e24.
173. Salman, B.I., et al., Ultrasensitive green spectrofluorimetric approach for quantification of Hg (II) in environmental samples (water and fish samples) using cysteine@ MnO2 dots. 2023. 38(2): p. 145-151.
174. Pramanik, R.J.C., A review on fluorescent molecular probes for Hg2+ Ion detection: mechanisms, strategies, and future directions. 2025. 10(7): p. e202404525.
175. Yao, W., et al., Sulfhydryl functionalized carbon quantum dots as a turn-off fluorescent probe for sensitive detection of Hg 2+. 2021. 11(57): p. 36310-36318.
176. Xiang, J., et al., Synthesis of Carbon dots from Biomass Chenpi for the Detection of Hg 2+. 2023. 11(10).
177. Harrison, R., Lead pollution: causes and control. 2012: Springer Science & Business Media.
178. Gupta, A., et al., Paper strip based and live cell ultrasensitive lead sensor using carbon dots synthesized from biological media. 2016. 232: p. 107-114.
179. Dhaffouli, A.J.M.J., Eco-friendly nanomaterials synthesized greenly for electrochemical sensors and biosensors. 2025: p. 115051.
180. Badran, A.M., et al., Advancements in adsorption techniques for sustainable water purification: a focus on lead removal. 2023. 10(11): p. 565.
181. Al-Saidi, H.M.J.C.P., Recent advancements in organic chemosensors for the detection of Pb2+: a review. 2023. 77(9): p. 4807-4822.
182. Kumar, A., et al., Green synthesis of carbon dots from Ocimum sanctum for effective fluorescent sensing of Pb2+ ions and live cell imaging. 2017. 242: p. 679-686.
183. Bandi, R., et al., Green synthesis of highly fluorescent nitrogen–Doped carbon dots from Lantana camara berries for effective detection of lead (II) and bioimaging. 2018. 178: p. 330-338.
184. Ansi, V., N.J.S. Renuka, and A.B. Chemical, Table sugar derived Carbon dot–a naked eye sensor for toxic Pb2+ ions. 2018. 264: p. 67-75.
185. 1Liu, Z., et al., Ratiometric fluorescent sensing of Pb2+ and Hg2+ with two types of carbon dot nanohybrids synthesized from the same biomass. 2019. 296: p. 126698.
186. Goel, A., et al., A multi-responsive pyranone based Schiff base for the selective, sensitive and competent recognition of copper metal ions. 2021. 249: p. 119221.
187. Elkhatat, A.M., et al., Recent trends of copper detection in water samples. 2021. 45(1): p. 218.
188. Chauhan, P., et al., Usage of coconut coir for sustainable production of high-valued carbon dots with discriminatory sensing aptitude toward metal ions. 2020. 16: p. 100247.
189. Praneerad, J., et al., Multipurpose sensing applications of biocompatible radish-derived carbon dots as Cu2+ and acetic acid vapor sensors. 2019. 211: p. 59-70.
190. Balakrishnan, T., et al., Formation mechanism and application potential of carbon dots synthesized from palm kernel shell via microwave assisted method. 2022. 5(2): p. 150-166.
191. Intakes, S.C.o.t.S.E.o.D.R., et al., Dietary reference intakes for vitamin A, vitamin K, arsenic, boron, chromium, copper, iodine, iron, manganese, molybdenum, nickel, silicon, vanadium, and zinc. 2002: National Academies Press.
192. Shander, A., M. Cappellini, and L.J.V.s. Goodnough, Iron overload and toxicity: the hidden risk of multiple blood transfusions. 2009. 97(3): p. 185-197.
193. Korchef, A., et al., Iron removal from aqueous solution by oxidation, precipitation and ultrafi ltration. 2009. 9(1-3): p. 1-8.
194. Shahbaz, M., et al., Fluorescent/Photoluminescent Carbon Dots as a Sensor for the Selective and Sensitive Detection of Fe3+/Fe2+ Metal Ions. A Review of the Last Decade. 2025: p. 1-24.
195. Song, Y., et al., Green fluorescent nanomaterials for rapid detection of chromium and iron ions: wool keratin-based carbon quantum dots. 2022. 12(13): p. 8108-8118.
196. Zhao, P., et al., Facile and green synthesis of highly fluorescent carbon quantum dots from water hyacinth for the detection of ferric iron and cellular imaging. 2022. 12(9): p. 1528.
197. Bahadır, Z., et al., Separation and preconcentration of lead, chromium and copper by using with the combination coprecipitation-flame atomic absorption spectrometric determination. 2014. 20(3): p. 1030-1034.
198. Wang, N., et al., Visible light photocatalytic reduction of Cr (VI) on TiO2 in situ modified with small molecular weight organic acids. 2010. 95(3-4): p. 400-407.
199. Yang, W.-M., et al., Efficient reduction of Cr (VI) with carbon quantum dots. 2022. 7(27): p. 23555-23565.
200. Tyagi, A., et al., Green synthesis of carbon quantum dots from lemon peel waste: applications in sensing and photocatalysis. 2016. 6(76): p. 72423-72432.
201. Tohamy, H.A.S., M. El-Sakhawy, and S.J.J.o.F. Kamel, Eco-friendly synthesis of carbon quantum dots as an effective adsorbent. 2023. 33(2): p. 423-435.

## Author(s) Bio

**Muhammad Arslan Akhtar** received his Master's degree in Chemistry from COMSATS University Islamabad. His research interests focus on the synthesis, characterization, and applications of carbon quantum dots, particularly for sensing applications. He has published two research articles in Q1 journals and is the author of three review articles in this field. He has extensive research experience in carbon quantum dot–based nanomaterials.
Email: arslanimran042@gmail.com

**Jalwa Anum** received her Master's degree in Chemistry from COMSATS University Islamabad. Her research interests include the green synthesis, characterization, and sensing applications of carbon quantum dots. She has published two research articles in Q1 journals related to carbon quantum dots and has gained solid research experience in nanomaterial-based sensing systems.
Email: jilashah444@gmail.com

**Abdul Rehman** obtained his Bachelor's degree in Chemistry from Government College University Faisalabad. He is currently pursuing his Master's degree in Chemistry at the Institute of Molecular Plus, Tianjin University, China. His research focuses on the synthesis of nanomaterials, chemical sensors, and electrocatalysis. He has published a review article in *Nano Research*.
Email: abdul372r@gmail.com

**Rabia** obtained her Bachelor's degree in Applied Chemistry from GC University Faisalabad, Sahiwal Campus. She is currently pursuing her Master's degree in Chemistry at the Institute of Molecular Aggregation Science, Tianjin University, China. Her research focuses on the development of chemical sensors, and she has published one review article in *Chemical Research in Chinese Universities (CRCU)*.
Email: rabiaabdulshakoor4@gmail.com